PERIOD-DOUBLING CASCADES
IN ONE AND TWO PARAMETER MAPS

by

Vandana Saini
A Dissertation
Submitted to the
Graduate Faculty
of
George Mason University
In Partial fulfillment of
The Requirements for the Degree
of
Doctor of Philosophy
Mathematics

Committee:

_____	Dr. Evelyn Sander, Committee Chair
_____	Dr. Daniel Anderson, Committee Member
_____	Dr. Maria Emelianenko, Committee Member
_____	Dr. Paul So, Committee Member
_____	Dr. David Walnut, Department Chair
_____	Dr. Donna Fox, Associate Dean for Student Affairs, College of Science
_____	Dr. Fernando Miralles-Wilhelm, Dean, College of Science

Date: _____ Fall Semester 2020
George Mason University
Fairfax, VA

Period-Doubling Cascades in One and Two Parameter Maps

A dissertation submitted in partial fulfillment of the requirements for the degree of Doctor of Philosophy at George Mason University

By

Vandana Saini
Master of Science
George Mason University, 2012
Master of Science
Panjab University, 2008

Director: Dr. Evelyn Sander, Professor
Department of Mathematical Sciences

Fall Semester 2020
George Mason University
Fairfax, VA

Dedication

I dedicate this dissertation to my parents. Without their efforts and hard work I would not be where I am today.

Acknowledgments

I would like to thank my advisor, Dr. Evelyn Sander who made this possible. I could not have asked for a better advisor. I am sincerely grateful to her for being so patient with me and for always supporting me.
I would like thank the rest of thesis committee, Dr. Daniel Anderson, Dr. Maria Emelianenko and Dr. Paul So for their encouragement and insightful comments.
I would like to thank my family. I could not have done this without their help, support and encouragement. I would like to thank my husband for supporting me all these years and for constantly encouraging me to do my best.

Table of Contents

List of Tables

List of Figures

Abstract

PERIOD-DOUBLING CASCADES IN ONE AND TWO PARAMETER MAPS

Vandana Saini, PhD

George Mason University, 2020

Dissertation Director: Dr. Evelyn Sander

Period doubling cascades are one of the most prominent features of one-parameter families of maps, $F : \mathbb{R} \times \mathcal{M} \to \mathcal{M}$, where $\mathcal{M}$ is a locally compact manifold without boundary, typically $\mathbb{R}^N$. This dissertation is divided into two parts. In the first part period doubling cascades in one parameter maps are considered. In the second part we consider the implications of period doubling cascades in maps with two parameters.

Our first set of results builds on 60 years of history of period doubling cascades in one parameter families. It has been previously proved that under certain conditions on a family of maps, cascades persist even under large perturbations in one dimensional maps and in coupled quadratic maps. We extend this work to prove that the cascades persist if we couple N one dimensional maps which satisfy certain conditions with a coupling g. Then, we use this result to prove the existence of cascades for a coupled family of cubic maps and for a mixed family of quadratic and cubic maps. Based on an established method for enumerating the period of a cascade, we are able to enumerate the cascades for a series of concrete examples including degree five and degree six polynomial maps.

In the second part, we concentrate on results for period doubling cascades in two parameter families of maps. Starting with the work of Milnor it has been observed that when a bifurcation diagram for a map with multiple extrema is drawn in the parameter space, it is seen to contain many shrimp-like

structures. A shrimp in the two parameter space can be viewed as a counterpart of a stable periodic window in one parameter bifurcation diagram. Many different methods have been used to investigate the parameter space like isoperiodic diagrams, continuation methods and the Lyapunov graph method. We use information from the first part of this dissertation to conclude results for the previously discussed shrimps for the cubic map. We demonstrate that shrimps occur in degree five and degree six polynomial maps derived in the first part of this dissertation. We show that the shrimps appear in the parameter space for the values of the parameters where a stable periodic window appears in the bifurcation diagram. In the past shrimps have not been observed in the quadratic map. We also compare the bifurcation diagram and the Lyapunov graph of a population model with three parameters and show that typical shrimps do not exist in its parameter space. We conjecture that a typical unimodal map does not have shrimps with multiple legs.

Chapter 1: Introduction

Period-doubling cascades have been observed in a wide array of physical, biological, and chemical experiments, as well being common in dynamical systems varying with a parameter. In particular, a cascade is an infinite sequence of period doubling bifurcations, resulting in periodic orbits with periods limiting to infinity. Quite notably, they are usually observed to occur during the transition from order to chaos. Period-doubling cascades were first reported by Myrberg in 1962 [38], and rediscovered by Robert May in [28], whose work widely popularized them throughout science.

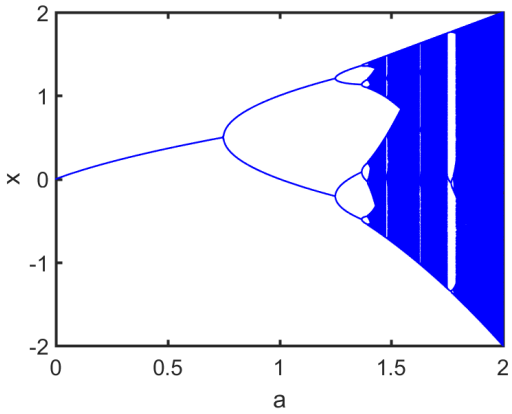

Figure 1.1: Bifurcation diagram for the quadratic map $q(a, x) = a - x^2$

Feigenbaum [35–37] examined the limiting behaviour of one dimensional period doubling cascades. Using renormalization theory, he was able to derive universal spatial and parameter scalings which are valid for a wide class of one dimensional maps. His results have been extended to higher dimensional maps in [40]. The most familiar case of cascades occurs for the quadratic map $q(a, x) = a - x^2$. This map has an infinite number of cascades, and all period doublings occur for a increasing (See Figure 1.1). This follows from a result of Milnor and Thurston [32], which

states that for this map, periodic orbits are never destroyed as a increases. This monotonicity result was originally proved by Douady and Hubbard and in [3], the authors have recently proved the Milnor's Monotonicity conjecture using real analysis. In this case, the existence of cascades has been proved on the basis of the property of monotonicity. This method of proof cannot be used in the general cases, since many cascade-possessing families do not have the monotonicity property. One-dimensional families do not always display monotonicity, and higher dimensional systems are typically non-monotonic as shown in [22].

Yorke and Alligood [53] used topological methods to prove that attracting periodic orbits of all periods appear in the process of creation of a horsehoe. In particular they showed the existence of period doubling cascades in maps satisfying a set of conditions. Extending these results, Sander and Yorke [47] studied general N-dimensional families under certain hypotheses. Large scale perturbations of one dimensional maps with cascades were studied in [47]. They developed a series of general criteria for the existence of cascades in the context of parametrized maps and explained why the cascades appear with infinite multiplicity. Note that both the methods used and conclusions reached are different than those obtained via renormalization theory. Sander and Yorke proved that in the case of parameterized one-dimensional quadratic

$$q(\lambda, x) = \lambda - x^2 + g(\lambda, x)$$

cubic maps

$$c(\lambda, x) = x^3 - \lambda x + g(\lambda, x)$$

and quartic

$$quart(\lambda, x) = x^4 - 2\lambda x^2 + \lambda^2/2 + g(\lambda, x),$$

where λ and $x \in \mathbb{R}$, and $g : \mathbb{R} \times \mathbb{R} \to \mathbb{R}$, for each generic, smooth, C^1-bounded function g, the maps have exactly the same number of unbounded period-k cascades as occur in the case $g \equiv 0$. In addition the number of cascades is infinite. A large scale perturbation in the context of these maps can be any smooth, C^1 bounded function and can be arbitrarily large. These large scale perturbation

results are also shown for an N-dimensional family of coupled quadratic maps.

In Chapter 2, we generalize this N-dimensional result to a family of coupled maps with k-horseshoes where k is not necessarily the same for each map. We specifically verify that cubic maps have 3-horseshoes, and therefore the results hold for a coupled family with any combination of N cubic maps. We also count the number of period-k cascades for a mixed coupled family of cubic and quadratic maps. For example, in Figure 1.2, the periodic orbits and the bifurcation diagram of the one-dimensional cubic map $f(r, x) = rx - x^3 + c\sin x + c$ are shown. It can be seen that the cubic map for the case $c = 0$ has a pitchfork bifurcation at $\lambda = 1$, but by introducing a small perturbation (in Hausdorff metric, refer to Chapter 2 for definition) when $c = 0.15$ and $c = 1$ the symmetry is broken and the pitchfork bifurcation is replaced by a stable branch and a saddle node bifurcation. In Figure 1.3, the bifurcation diagrams for coupled cubic maps $F(\lambda, (x, y)) = (-x^3 + \lambda x + d\sin y + d, -y^3 + 1.1\lambda y + c\cos x + c)$, where λ is the parameter and $c = 0.01$ and $d = 0.15$ are constants. The stable set of a mixed family of coupled maps is also shown $F(\lambda, (x, y)) = (-x^2 + \lambda + d\cos y + d, -y^3 + (\lambda + 2)y + c\cos x + c)$, where $c = 0.01$ and $d = 0.38$.

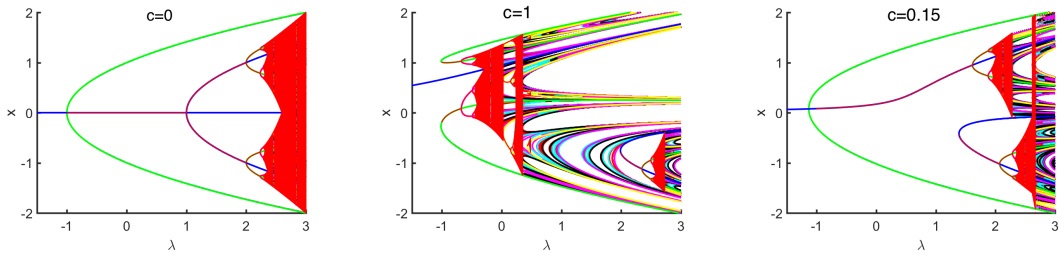

Figure 1.2: Periodic orbits (periods 1 through 8 in colors) and bifurcation diagrams (in red) of cubic map $f(\lambda, x) = -x^3 + \lambda x + c\sin x + c$, where $c = 0, 1, 0.15$. The periodic orbits are calculated using contour in Matlab. The cubic map $f(\lambda, x)$ with $c = 0$ has a pitchfork bifurcation. By introducing a small perturbation, the pitchfork bifurcation is replaced by a stable branch and a saddle node bifurcation.

In [21], the enumeration scheme was quantified for abstract symbolic of transitions to full k-shifts which we refer to as k-**map** defined in Definition 2.1.5. In Chapter 2, we illustrate this for a

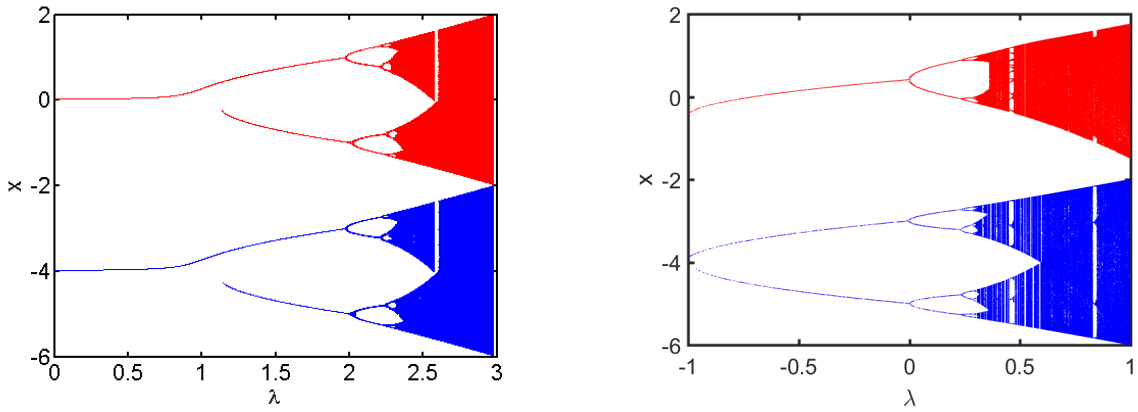

Figure 1.3: Coupled maps: The left figure shows x and y in the stable set as a function of parameter λ for the system of cubic maps $F(\lambda,(x,y)) = (-x^3+\lambda x+d\sin y+d, -y^3+1.1\lambda y+c\cos x+c)$, where $c = 0.01$ and $d = 0.15$. The right figure shows x and y in the stable set as a function of parameter λ for the mixed system of quadratic and cubic maps $F(\lambda,(x,y)) = (-x^2+\lambda+d\cos y+d, -y^3+(\lambda+2)y+c\cos x+c)$, where $c = 0.01$ and $d = 0.38$. When a perturbation is introduced to the cubic map, the pitchfork bifurcation loses stability and is replaced by a stable branch and a saddle node bifurcation. For clarity of the picture the values of y have been displaced by 4 units below the values of x.

series of concrete examples where we can prove there are k-maps for $k = 2, 3, 5, 6$. For example, Figure 2.1 shows the bifurcation diagram for the cubic map $c(\lambda, x) = \lambda x - x^3$ which is a 3-map. We then enumerate the cascades of the coupled maps, and perform numerical experiments on some examples. Note that our coupling theorem allows for all coupled maps to be k-maps with the same k, or we can mix k-maps with different values of k, and we will still be able to give a count of the number of period-doubling cascades of each period.

This dissertation proceeds as follows: In Chapter 2 we prove that a family of N coupled k-maps, where k is not necessarily the same, has infinitely many cascades. Using results previously proved on enumeration, we also enumerate cascades for a series of k maps where $k = 2, 3, 5,$ and 6. In Chapter 3, we give results for two parameter families of maps which have infinitely many cascades. Specifically we relate the results from Chapter 2 to the dynamics observed in two parameter families of maps.

Chapter 2: Period doubling cascades in one parameter maps

In this chapter, we concentrate on one parameter families of maps. We prove that under certain conditions on a family of maps, cascades persist even under large perturbations. Such results have already been considered by Sander and Yorke [47]. We extend these results to prove the existence of cascades for coupled families of cubic maps, for a mixed family of certain quadratic, cubic, quartic, quintic and degree six maps. In each case we count the number of cascades of each finite period. We generalize the set of functions for which the hypotheses of the cascades theorem hold to coupled systems beyond quadratic. In particular, we consider

$$F : \mathbb{R} \times \mathbb{R}^N \to \mathbb{R}^N,$$

where $F = (F_1, F_2, \ldots, F_N)$, and

$$F_i(\lambda, x_1, \ldots, x_N) = f_i(\lambda, x_i) + g_i(\lambda, x_1, \ldots, x_N),$$

where each f_i is a one-dimensional parametrized k-*map*. Thus, we are considering the coupling of N one-dimensional maps with coupling g. We will give a formal definition subsequently, but roughly speaking, a parametrized k-map has the property that for all sufficiently small parameter values, there is only non-chaotic behavior with a finite number of periodic orbits, whereas for all sufficiently large parameter values, there is dynamics which is topologically conjugate to a full shift on k symbols. This implies that each uncoupled map ($g = 0$) undergoes infinitely-many period-doubling cascades as the parameter increases. When we couple such maps weakly (corresponding to small g), we might expect that the system also undergoes (infinitely many) period-doubling cascades. In fact this is true even for non-weak coupling (meaning g is large). We can be more precise about the nature of the cascades: there is a method for enumerating the period of a cascade, and

in this numbering scheme, cascades will maintain the same periods as for the original mapping. In [21], an enumeration scheme was quantified for abstract symbolic of transitions to full k-shifts. In this chapter, we illustrate this for a series of concrete examples where we can prove there are k-maps meaning that its conjugate to full shift on k-symbols as defined in Definition 2.1.5 for $k = 2, 3, 5, 6$. For example, Figure 2.1 shows the bifurcation diagram for the cubic map $c(\lambda, x) = \lambda x - x^3$ which is a 3-map. We then enumerate the cascades of the coupled maps. Note that our coupling theorem allows for all coupled maps to be k-maps with the same k, or we can mix k-maps with different values of k, and we will still be able to give a count of the number of period-doubling cascades of each finite period.

Before going into detail of our results, we give some background on prior results. Work on cascades for the cubic map goes back to Robert May [29], who considered the application of cubic maps in population dynamics and in experiments with electronic circuits. In [31], Milnor studied a certain family of cubic maps in both real and complex domains. Namely, Milnor considered the two parameter family of cubic maps $x \to \sigma x^3 - 3Ax + \sqrt{|B|}$ where A and B are real constants and $\sigma = \pm 1$ is the sign of the leading coefficient. He observed that in the two-parameter bifurcation diagram, there are swallow shaped regions, arch shaped regions, and product like regions, where the regions are determined by their stable dynamics. He explains these regions using renormalization theory. In [20], the authors studied the bifurcation diagrams of periodic orbits of smooth scalar maps with one and two-dimensional parameter spaces. Specifically, they looked at windows of periodic behavior within the chaotic region of parameter space. They also proved that there exists a canonical family of maps such that the bifurcations within a periodic window of a given map can be approximated by a linear transformation of the bifurcation diagrams of the canonical map. In [23], the authors have proved the existence of periodic orbits without finding trapping regions for the periodic orbits and without establishing a priori upper bounds on the periods of orbits. In particular, they used one-forms get around some of the technical issues in order to discuss existence of periodic orbits. In contrast, we work on proving the existence of period-doubling cascades and we consider families with generic bifurcations. Period doubling route to chaos has also been studied in impulsive systems [13]. It has been proved that the impulsive response system replicates the sensitivity and

the period-doubling cascade of the drive. As mentioned previously, period-doubling cascades are

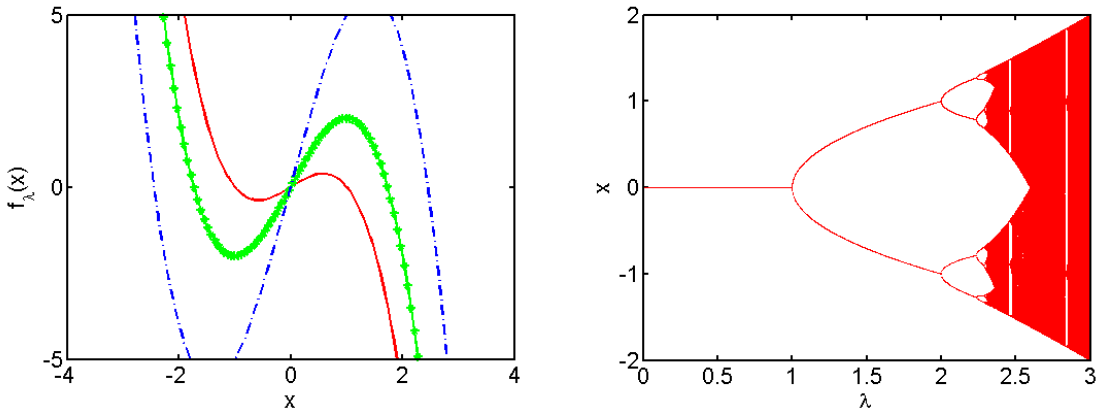

Figure 2.1: In the left picture a graph of the parametrized cubic map $f(\lambda, x) = \lambda x - x^3$ is shown for $\lambda = 1, 3, 6$. For each value of λ, the attracting set for $f(\lambda, x)$ in $[-2, 2]$ is shown in the right picture. There are infinitely many period-doubling cascades.

shown to occur in the transition from order to chaos. Since we are using topological methods, we are able to achieve results even if we only consider one aspect of chaos versus order, and that is the number of periodic orbits. In particular, previous results guarantee the existence of infinitely-many cascades whenever there are two parameters such that at one parameter, there is *order* in that there are a finite number of periodic orbits, and at the second parameter, there is *chaos* in the sense that there are an infinite number of periodic orbits and there is rapid growth rate of the number of periodic orbits as a function of the period. To be more specific, we introduce the concept of *periodic orbit entropy*.

Definition 2.0.1. Let S_p be the number of periodic points of period p, then the periodic orbit entropy is the exponential growth rate of orbits with respect to period, given by

$$h = \limsup_{p \to +\infty} \frac{\log S_p}{p} .$$

This is closely related to positive topological entropy. In some cases periodic orbit entropy is equal to topological entropy. For interval maps, Misiurewicz and Szlenk [34] proved that for a

continuous and piecewise monotone map of the interval the topological entropy is bounded above by the exponential growth rate of the number of periodic orbits which is periodic orbit entropy. See [46] for a detailed discussion. The topological entropy h for the quadratic map is a monotone function of the parameter. Proofs of this result can be found in [11, 30, 32]. Milnor (see [31]), conjectured that the set of parameters within a family of real polynomial interval maps, for which the topological entropy is constant is connected. Milnor and Tresser [33] proved this conjecture for the cubic case and the general case was proved by Bruin and Strien in [7]. This implies that topological entropy is monotone in these cases. However, this is not true in general, see [48]. Even though topological entropy measures the complexity of the system, it does not give much information about the period doubling cascades or their enumeration.

We now introduce our cascade enumeration scheme. Although there are infinitely many cascades, it is possible to enumerate them by classifying them in terms of their period. In particular, a cascade from a period-k is a connected set of period orbits in phase cross parameter space such that the bifurcation orbits contain branches of period $k, 2k, 4k, ...$ all lying in the bounded region of parameter and phase space. Note that often, cascades are considered for period doublings for stable periodic orbits, since stable orbits are the most easy to observe dynamically, but in fact in dimension larger than one, cascades branches can also be period doubling bifurcations in which all periodic orbits are unstable. In this chapter our primary interest is not stability of cascades but rather showing that period doubling cascades exist for families of N coupled maps and enumerating them.

We consider only maps F which are generic in the sense that all its bifurcation orbits are generic. A bifurcation orbit is generic if it is one of the following three types:

- A generic saddle node bifurcation
- A generic period-doubling bifurcation
- A generic Hopf bifurcation for such that at the bifurcation no eigenvalue of the Jacobian is a root of unity.

We say F is generic when each of its bifurcation orbits is generic. In particular, such maps F are dense in set of C^∞ families (and in fact this is also true in the space of C^k families for all k

sufficiently large), see [47].

We proceed as follows: In section 2.1 we give notation and previous results that we use to prove our result. In section 2.2, we give a general result on the existence of cascades. The result is based on prior work, but carefully adapted to be in the proper form for considering the coupling of k-maps. In section 2.3, we prove the case of N-coupled cubic maps. In section 2.4, we consider a mixed family of quadratic and cubic maps and use the results of [21] to count the number of cascades of period k for each k. In Section 2.5, we give examples of one-dimensional parametrized k-maps for $k = 5, 6$. These are specially chosen degree 5 and degree 6 polynomials such that period doubling cascades are preserved under large perturbation. In particular, these maps extend the set of N-dimensional maps we can couple together and still guarantee cascades.

2.1 Background

Notation and statements of the results used are given in this section. All notations and definitions have been taken from [21] and [47]. We assume the following conditions are satisfied by smooth one-parameter families of maps:

Hypothesis 1 Let $\mathcal{M}$ be a smooth n-dimensional locally compact manifold. Let $F : \mathbb{R} \times \mathcal{M} \to \mathcal{M}$ be C^∞ - smooth. This is referred to as a parametrized map on $\mathcal{M}$.

A period-k orbit of a parametrized map $F : \mathbb{R} \times \mathcal{M} \to \mathcal{M}$ is a **flip** orbit if the number of eigenvalues of its Jacobian matrix, $D_x F^k(\lambda, x)$ less than -1 is odd, and -1 is not an eigenvalue. Otherwise the orbit is **regular**. Denote the space of regular orbits of F in $\mathbb{R}\times\mathcal{M}$ under the Hausdorff metric by $Reg(F)$. The distance between two orbits in the space $Reg(f)$ is defined using the Hausdorff metric. Two orbits are close in $\mathcal{M}$ if every point of each orbit is close to some point of the other orbit. Refer to formal definition in Section 2 of [47].

Definition 2.1.1. (**Component**) A set $C \subset \mathbb{R} \times \mathcal{M}$ is defined to be a set of orbits if $(\lambda, x) \in C$ implies that x is a periodic point of $F(\lambda, .)$; and in addition, every other point (λ, x') on the same orbit is also in C. We say that a set of orbits C is a component if it satisfies the following properties:

(i) C contains only regular orbits (meaning no flip orbits).

(ii) C is path connected; that is for any two points (λ_a, a) and (λ_b, b) in C, there is a path of periodic points all of which are contained in C, such that one end of the path is (λ_a, a) and the other end is (λ_b, b). Furthermore, there is an upper bound on the periods of the periodic points on the connecting path. (The periods of orbits in a component are unbounded in the cases we consider).

(iii) C is maximal, in the sense that it is not contained in a strictly bigger set of orbits satisfying (i) and (ii).

Note that each regular periodic orbit is contained in a component.

An **arc** is a set that is homeomorphic to an interval. We call it an **open arc** if the interval is open or half open if that describes the interval. An arc is called **bounded** if there is a compact subset of $\mathbb{R} \times \mathcal{M}$ that contains all of its orbits. Otherwise, it is called **unbounded**.

Definition 2.1.2. (**Paired cascades**) If a component is a bounded open arc, then it always contains two disjoint cascades, and are referred to as **paired cascades**.

Definition 2.1.3. (**Cascade component**) We define a **cascade component** as the following type of subarc of an open arc $\boldsymbol{A}$: Let k denote the smallest period of the orbits in $\boldsymbol{A}$. A cascade is a half-open subarc that contains orbits with all of the periods $k, 2k, 4k, 8k, ...$ such that it contains precisely one branch of orbits of period k. We refer to such a cascade as a **period-k cascade component**.

Typically this branch of period-k cascade on end of the parameter interval ends in a saddle node bifurcation and on the other end ends in period doubling bifurcations. This is typical for a quadratic map and is usually true for other maps as well.

Definition 2.1.4. (**Periodic window**) An interval of parameter values for which the only attractor is a periodic orbit is called a **periodic window** in the bifurcation diagram. A period-n window begins with a period-n saddle node bifurcation [2].

In Chapter 3, we are only considering stable behavior and therefore will only consider stable periodic windows. (See Figure 3.5 for an example.)

Definition 2.1.5. ($k-$**shift horseshoe map or** k**-map** in one dimension) We call a C^1 one dimensional function $G : \mathbb{R} \to \mathbb{R}$ a k**-map** when it has the following properties:

- there is a closed interval J and k non empty disjoint intervals $J_1 \subset J, J_2 \subset J, ..., J_k \subset J$ such that $G(J_1) = G(J_2) = ... = G(J_k) = J$; and

- $G(x) \in J$ implies $x \in \bigcup_{i=1}^{k} J_i$.

Note that these two conditions are equivalent to saying when G is restricted to the points which stay in J under iterations, it is equivalent to the full shift on k-symbols.
In the vast majority of results we explore the relations between the k-maps and the other concepts defined above.

A periodic orbit is either a **hyperbolic orbit**, meaning that there are no eigenvalues of norm one, or it is called a **bifurcation orbit**.

The next definition states the assumption that all the bifurcations are generic codimension-one bifurcations.

Definition 2.1.6. (Generic orbit bifurcations). Let $F : \mathbb{R} \times \mathcal{M} \to \mathcal{M}$ be C^∞ smooth. A bifurcation orbit P of F is **generic** if it is one of the following three types (as described in [44]):

(i) A generic saddle node bifurcation.

(ii) A generic period doubling bifurcation.

(iii) A generic Hopf bifurcation with complex conjugate eigenvalues of the Jacobian which are not roots of unity.

We say F is **generic** if each non-hyperbolic orbit is one of the above three types.

Hypothesis 2 (Generic bifurcations) Assume Hypothesis 1. Assume that each orbit of F is either hyperbolic or is a generic bifurcation orbit.
There is a residual set of smooth parametrized maps which satisfies Hypothesis 2. See [47].

The next assumption states that the periodic orbits are contained in a bounded set. The region is bounded by the parameter values λ_0 and λ_1 and its assumed that there are no bifurcations of periodic orbits on the boundary.

Hypothesis 3 (Orbits near the boundary) Let F satisfy Hypothesis 2. Let $\lambda_0 < \lambda_1$, and let $U = [\lambda_0, \lambda_1] \times \mathcal{M}$. Assume that all orbits in $\mathcal{M}$ for $F(\lambda_0, \cdot)$ and $F(\lambda_1, \cdot)$ are hyperbolic. Assume that all orbits in U are contained in a compact subset of $\mathcal{M}$. A cascade is **essentially in** U if all but a finite number of its bifurcation orbits are in U.

Definition 2.1.7. (Expansive map) A homeomorphism f from the compact metric space M onto M is expansive if there exists $\alpha > 0$, such that if $x, y \in M$ and $dist(f^n(x), f^n(y)) \leq \alpha$ for every integer n, then $x = y$.

A sufficient condition for a diffeomorphism to be expansive is that all the eigenvalues of the derivative matrix have absolute values greater than 1. Therefore, as a consequence of these definitions we can show that a differomorphism G on $\mathbb{R}^N$ is expansive by showing that $\left|\left|DG^{-1}\right|\right| < 1$ for all $x \in S$, where $||.||$ denotes the operator norm.

Definition 2.1.8. (Orbit Index) Assume y to be a hyperbolic orbit of order p of a smooth map G.

Let σ^+= number of real eigenvalues (with multiplicity) in $(1, \infty)$ and σ^-= number of real eigenvalues (with multiplicity) in $(-\infty, -1)$. Then, the orbit index is defined to be $\phi([x]) = (-1)^{\sigma^+}$ if σ^- is even and is 0 if σ^- is odd. Refer to [47] for a complete definition.

Definition 2.1.9. Assume Hypothesis 3. Let $p \in Reg(F)$ be a hyperbolic orbit for F at one of the ends of the parameter interval. That is, either $\lambda = \lambda_0$ or λ_1. The orbit p is called an **entry orbit** for $\lambda = \lambda_0$ if the number of real eigenvalues greater than +1 is even, and for $\lambda = \lambda_1$ if the number of real eigenvalues greater than +1 is odd. Otherwise, it is called an **exit orbit**.

In [47], Sander and Yorke developed general criteria for the existence of cascades and explained why an infinite number of cascades appear during the formation of horseshoes. The following theorem is the main result of [47].

Theorem 2.1.10. ***(Cascades from boundaries)*** *Assume Hypothesis 1-3. Let K = number of entry orbits and J = number of exit orbits. Also assume $|K - J| \neq 0$. We allow one but not both of the sets to have an infinite number of elements.*

(C_K) If $K < J$, then all but possibly K orbits are contained in distinct components, each of which contains a cascade essentially in U. Likewise, if $J < K$, then all but possibly J orbits are contained in distinct components, each of which contains a cascade essentially in U.

(C_0) If $J = 0$ or $K = 0$, then the regular orbits of ∂U are in one-to-one correspondence with the components that intersect the boundary. Each of these components has one cascade that is essentially in U.

As corollaries of this result, Sander and Yorke, in [47], proved the existence of infinitely many cascades for large perturbations of parametrized families of quadratic and cubic maps and also counted the number of cascades for each period k by counting the number of regular orbits. In this chapter we provide more examples, namely, a degree 5 and degree 6 family of parametrized maps for which this result holds and show that they have infinitely many cascades.

Sander and Yorke, in [47] also proved that a system of N quadratic maps plus a coupling term has infinitely many cascades and calculated the number of period-k cascades for each period-k. In this chapter we prove and extend this result to N coupled maps with k-horseshoes and k is not the same for each map. We then show it is true for the case of N coupled cubic maps and also for a mixed family of maps. In [21], Joglekar, Sander and Yorke proved the existence of cascades and also gave a way to enumerate the cascades as a function of the periodic orbits from which they arise. In particular they show that it is sufficient to count the number of regular periodic orbits by proving that the number of regular periodic orbits is approximately half of the total number of periodic orbits. Thus, if there are infinitely many of one, there are infinitely many of the other. They give a recursive formula for the number of regular periodic orbits of an m-shift. In this dissertation we apply the results of [21] to count the number of cascades of a mixed family of quadratic and cubic maps. Our main result gives generalization of the results of [47] and [21]. We first prove the general statement and then apply it to concrete examples.

Theorem 2.1.11. ***General case of N-dimensional coupled system*** *Let $f_i : \mathbb{R} \times \mathbb{R} \to \mathbb{R}$ be a C^∞ smooth map, such that $\lim_{\lambda \to \pm\infty} f_i = \pm\infty$ for each $i = 1, 2, ...N$. List of assumptions:*

(a) Assume that all of bifurcation orbits of each f_i are generic bifurcation orbits.

(b) Assume that for λ sufficiently small each f_i has a finite number of periodic orbits and for λ sufficiently large there are infinitely many periodic orbits.

(c) Assume that for sufficiently large value of λ, f_i is a k-map on the maximal bounded invariant set of f_i and on this set the map f_i is expansive.

Then, each f_i has infinitely many cascades and the cascades are preserved under perturbations. This result for one dimensional maps is proved in [21]. We introduce a coupling term to this family of maps, $g_i(\lambda, x_1, x_2, ..., x_N)$ where g is such that for some $\beta > 0$ $\|g(\lambda, 0)\| < \beta$ and $\|D_x g(\lambda, x)\| < \beta|x|$ and g is smooth. These properties on g guarantee that when $|\lambda|$ is large, the behavior of individual maps f_i dominates the coupling between the maps. Let g be such that F has generic bifurcations, and if we define

$$F_i = f_i(\lambda, x_i) + g_i(\lambda, x_1, x_2, ..., x_N),$$

where $g = (g_1, g_2, ..., g_N)$ satisfies the above mentioned conditions, the coupled map $F = (F_1, F_2, ..., F_N)$ is a family of generic maps and F has infinitely many period doubling cascades. Note that g can be any smooth function and can be arbitrarily large as long as it satisfies the above mentioned conditions. We can also count the number of period-k cascades for each k. This result is proved in section 2.2.

2.2 Proof of General case

Proof will be divided into the following two propositions: (1) For sufficiently small λ_0, there are only a finite number of periodic orbits or no periodic orbits for F. (2) For sufficiently large λ_1, if the maximal bounded invariant set of f_i is conjugate to a shift map on M_i symbols then the maximal

bounded invariant set (say A) of $F(\lambda_1, .)$ is conjugate to a shift map on product of $\prod_{i=1}^{N} M_i$ symbols. On this set, the map F is expansive on this invariant set A.

Proof of (1)

(i) Suppose that for a sufficiently small value of λ each f_i has no periodic orbits or a finite number of periodic orbits. Since $|g|$ and $|D_x g|$ are bounded, we can always find a value of λ sufficiently small so that the number of periodic orbits are not affected by the coupling term g. Therefore, if each f_i has no or finitely many periodic orbits for a fixed value of λ, we can find a value of $\lambda = \lambda_0$ sufficiently small for which F has no or finitely many periodic orbits.

Proof of (2)

We show the following estimates:

(ii) Assume for λ (fixed) sufficiently large, the maximal bounded invariant set of $f_i(\lambda, x_i)$ is conjugate to a shift map on M_i symbols and on this set $f_i(\lambda, x_i)$ is expansive. Therefore, $|\frac{\partial f_i}{\partial s}| > 1$ on all points in this set. For details see [47]. Consider the Jacobian matrix of $F(\lambda_1, x)$ where λ_1 is large.

$$D_x F = \begin{bmatrix} \frac{\partial f_1}{\partial x_1} + \frac{\partial g_1}{\partial x_1} & \frac{\partial g_1}{\partial x_2} & \cdots & \frac{\partial g_1}{\partial x_N} \\ \vdots & \vdots & \ddots & \vdots \\ \frac{\partial g_N}{\partial x_1} & \frac{\partial g_N}{\partial x_2} & \cdots & \frac{\partial f_N}{\partial x_N} + \frac{\partial g_N}{\partial x_N} \end{bmatrix}$$

Since the partial derivatives of g are bounded and $|\frac{\partial f_i}{\partial s}| > 1$. Therefore, the diagonal entries become arbitrarily large as we increase λ_1. Therefore, $D_x F$ is strictly diagonally dominant $(|a_{ii}| > \sum_{j \neq i} a_{ij})$. To prove that F is expansive on A we show for $u \in \mathbb{R}^n$, $|D_x F^{-1} u| < |u|$. Since $D_x F$ is strictly diagonally dominant, therefore $D_x F^{-1}$ exists. Also, since the diagonal entries are large for large λ, therefore by Gershgorin's theorem, we can conclude that the eigenvalues of $D_x F$ have absolute values greater than 1 as for a large value of λ the diagonal

entries are larger than the off diagonal entries, therefore the eigenvalues lie outside the unit circle and close to the diagonal entries. Therefore, $|D_xFv| = |ev| = |e||v| > |v|$, since $|e| > 1$. Let $u = D_xFv$. Then for some $v \in \mathbb{R}^n$

$$|D_xF^{-1}u| = |D_xF^{-1}D_xFv| = |v| < |D_xFv| = |u| \ .$$

Therefore, $|D_xF^{-1}u| < |u|$. Hence F is expansive on A.

(iii) For each i and for a fixed λ, let J_i be a closed interval such that $J_i = [-s_i, s_i]$ where s_i is finite and depends continuously on λ. It follows from assumption (c) that for each i there exists a finite number of disjoint closed intervals $A_{ij} \subset J_i$. Let $A_i = \bigcup_j A_{ij}$ then, for λ sufficiently large, the set $f_i(\lambda, \mathbb{R} \setminus A_i)$ contains no points of J_i. Let

$$J = J_1 \times J_2 \times ... \times J_N \text{ and } A = A_1 \times A_2 \times ... \times A_N \ .$$

Then at λ_1 the set $F(\lambda_1, \mathbb{R}^N \setminus A)$ contains no points of J.

Let $\beta_1 > 0$ be such that $|g_i(\lambda, 0)| < \beta_1$ and $\frac{\partial g_k}{\partial x_i}(\lambda, x) < \beta_1$ for every i and k. From the assumptions it is known that for $\lambda = \lambda_1$ sufficiently large, $f_i(\lambda_1, \mathbb{R} \setminus A_i)$ contains no points of J_i. Let $x \in J \setminus A$, then there is an i such that $x_i \in J_i$ and $x_i \in \bigcap_j A_{ij}^c$ for some i and j where A_{ij}^c is the complement of A_{ij}. Therefore, by the proof for one dimensional case, $f_i(\lambda_1, x_i)$ lies outside of J_i. Also, if $x \in \mathbb{R}^N \setminus J$ then for some i, $x_i \in \mathbb{R} \setminus J_i$, which implies $f_i(\lambda, x_i)$ lies outside J_i, and therefore $F(\lambda, x)$ is not in J.

(iv) Assume that for a sufficiently large λ there is a bounded set B_i which contains all periodic points of f_i for each i. Then the set $B = \prod_{i=1}^{N} B_i$ is bounded and contains all periodic points of F.

(v) For a sufficiently large value of λ, assume that $f_i(\lambda, A_{ij})$ maps diffeomorphically across J_i for

each i and j. Let A_{ij} be a component of A. Fix λ_1 be large enough that (a)-(c) hold. From (ii), there exists x_i in each J_i such that $f_i(\lambda_1, x_i) \in J_i$ for each i. Therefore $F(\lambda_1, A_{ij}) \cap J \neq \phi$.

Let $C = F(\lambda_1, A_{ij})$ for a fixed i, j. We prove that $J \subset C$ and F maps A_{ij} diffeomorphically on J. We have shown above that for λ_1, F maps $J \setminus A$ outside of J. Therefore, the boundary of C does not intersect the boundary of J. Also since F is a local differomorphism and D_xF is non singular on A_{ij}, therefore, F maps the interior of A_{ij} to an open set. Since A_{ij} is a compact set being a closed interval, C is also compact, therefore the boundary of C is the image of the boundary of A_{ij}. Let x be $\in C \cap J$. Let y be any point not in C. On the straight line segment from x to y, let w be the point closest to y that is in C. Then w is in the image of the boundary of A_{ij}, so w is not in J. Since x is in the convex set J but w is not, therefore y is not in J. Hence, no point outside of C is in J. That is, J is a subset of C.

The proof of (1) and (2) follow from these steps: From (ii)-(v), it follows that at λ_1 the map F is topologically conjugate to the full shift on $\prod_{i=1}^{N} M_i$ symbols associated with M^N rectangles A_{ij}. Also all orbits are hyperbolic. From (iii), it follows that at λ_0 there are no orbits or a finite number of orbits. If there are no orbits at λ_0, and infinitely many orbits at λ_1 then by part C_0 of Theorem 2.1.10 the result follows. If there are a finite number of regular (exit) orbits as λ_0 and infinitely many orbits at λ_1 then since the number of exit orbits is smaller than the number of regular orbits orbits at λ_1, therefore all but a finite number of regular orbits for $\lambda = \lambda_1$ are contained in distinct components, each of which contains a cascade. If there are a finite number of regular (entry) periodic orbits λ_0, then the result follows by a similar argument and by part C_k of Theorem 2.1.10.

2.3 N-coupled cubic maps

The cubic map $\lambda x - x^3$ forms a 3-horseshoe in a similar way as the quadratic map forms a 2-horseshoe. Therefore, as λ is increased, cascades are seen. For a largely negative λ there is only one orbit which is the fixed point at $x = 0$. Since the derivative is less than -1 for this orbit, therefore

for largely negative $\lambda = \lambda_0$, the orbit index is 0 and it is a flip orbit. As λ increases, 0 undergoes a (non-generic) pitchfork bifurcation in which two new period-1 orbits are created. By introducing a perturbation, we get a parametrized map in which the pitchfork bifurcation is replaced by a stable branch and a saddle node bifurcation. See Figure 1.2.

Define the three shift tent map $T_3(x)$ as

$$T_3(x) = \begin{cases} -3x & \text{if } x \in [0, 1/3] \\ 3x - 2 & \text{if } x \in [1/3, 2/3] \\ -3x + 2 & \text{if } x \in [2/3, 1] \end{cases}$$

See Figure 2.2. For positive integer N and $X = (x_1, x_2, x_3, ..., x_N) \in \mathbb{R}^N$, let $G : \mathbb{R}^N \to \mathbb{R}^N$ be the product of N 3-shift tent maps (T_3).

$$G = (T_3(x_1), T_3(x_2), ..., T_3(x_N)).$$

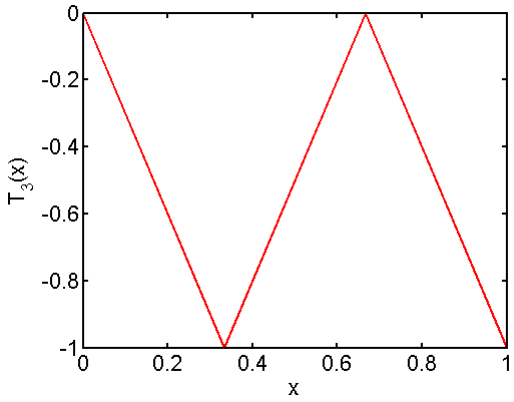

Figure 2.2: 3-shift tent map

In the following theorem, we show that the system of N coupled cubic maps has infinitely many cascades by proving that for a large value of λ this system is topologically conjugate to the shift

map on 3^N symbols.

Theorem 2.3.1. *Let $F : \mathbb{R} \times \mathbb{R}^N \to \mathbb{R}^N$ and $g : \mathbb{R} \times \mathbb{R}^N \to \mathbb{R}^N$ be C^∞ smooth and let each component F_i (for each $i = 1, 2, ..., N$) have the form*

$$F_i(\lambda, x_1, x_2, ..., x_N) = K_i(\lambda)x_i - x_i^3 + g_i(\lambda, x_1, x_2, ..., x_N)$$

where g is such that for some $\beta > 0$, $||g(\lambda, 0)|| < \beta$, $||D_x g(\lambda, x)|| < \beta|x|$. $K_i(\lambda)$ plays the role of λ. Then, for a residual set of g, for each positive integer $k \neq 2^m$ for $m \geq 0$, the number of unbounded cascades with period k is the same as the number of regular orbits for the map G.

Proof: Assume that g is such that F is generic. The proof of the theorem mimics the method of proof of corollary 4 from [47]. We divide the proof of the theorem into the following propositions:

Proposition 2.3.1. *For sufficiently small λ_0, $F(\lambda_0, .)$ has only one orbit, and that is an unstable fixed point.*

Proof. This follows from Corollary 4. There exists a parameter value λ_0 sufficiently negative that for any value of i, $i = 1, 2, ..., N$, there exists x_i, such that

$$K_i(\lambda_0)x_i - x_i^3 + g_i(\lambda_0, x_1, ..., x_N) = x_i$$

Also, since for each F_i, $F_i \to \infty$ as $x \to -\infty$ and $F_i \to -\infty$ as $x \to \infty$, therefore the fixed point x_i is unique for each F_i. Hence, there exists a unique fixed point $(x_1, x_2, ..., x_N)$ for $F(\lambda, x_1, x_2, ..., x_N)$. □

Proposition 2.3.2. *For all sufficiently large λ_1, $F(\lambda_1, .)$ is topologically conjugate to the full shift on 3^N symbols. We prove this fact by showing the following estimates. For λ_1 sufficiently large so that $K_i(\lambda_1) > 0$, let $s_i = \sqrt{K_i(\lambda_1)}$, $J_i = [-2s_i, 2s_i]$ and $J = J_1 \times J_2 \times ... \times J_N$. Define*

$$A = \left\{ \frac{2.5s}{3} \leq |x| \leq \frac{s}{3} \right\}.$$

For $j = 1, 2, ..., 3^N$, let A_j denote one of the 3^N connected components of $A \subset J$. We show the following estimates for λ_1 chosen sufficiently large:

1. *at λ_1, and for any point in A, $D_x F$ is diagonally dominant (i.e. $|a_{ii}| \geq \sum_{j \neq i} |a_{ij}|$ for all i) and the dynamics is expansive (A map F on $\mathbb{R}^N$ is said to be expansive on S if $\left|\left|DG^{-1}\right|\right| < 1$ for all $x \in S$, where $||.||$ denotes the operator norm).*

2. *At λ_1, the set $F(\lambda_1, \mathbb{R}^N \setminus A)$ contains no points of J.*

3. *There is a ball $B \subset \mathbb{R}^N$ s.t. for all $\lambda < \lambda_1$, each bounded trajectory is in B.*

4. *At λ_1, $F(\lambda, A_i)$ maps diffeomorphically across J for all i.*

Proof. 1. We show this to prove that the given map for sufficiently large λ is topologically conjugate to the shift map on 3^N symbols. $F_i(\lambda_1, x_1, x_2, ..., x_N) = K_i(\lambda_1)x_i - x_i^3 + g_i(\lambda_1, x_1, x_2, ..., x_N)$ The derivative is given by $F_i'(\lambda_1, x_1, x_2, ..., x_N) = K_i(\lambda_1) - 3x_i^2 + \frac{\partial g_i}{\partial x_i}$ This implies

$$D_x F = \begin{bmatrix} K_1(\lambda_1) - 3x_1^2 + \frac{\partial g_1}{\partial x_1} & \frac{\partial g_1}{\partial x_2} & \dots & \frac{\partial g_1}{\partial x_N} \\ \vdots & \vdots & \ddots & \vdots \\ \frac{\partial g_N}{\partial x_1} & \frac{\partial g_N}{\partial x_2} & \dots & K_N(\lambda_1) - 3x_N^2 + \frac{\partial g_N}{\partial x_N} \end{bmatrix}$$

Since the partial derivatives of g are bounded, we can choose λ_1 large enough so that

$$|a_{ii}| > \sum_{j \neq i} |a_{ij}| \text{ for all } i$$

Therefore, $D_x F$ is strictly diagonally dominant. And therefore, by a similar argument as in the proof of general statement we can show that F is expansive on A.

2. In this step we want to show that at λ_1, F maps each A_j onto J_i. To prove this we show at λ_1, $F(\lambda_1, \mathbb{R}^N \setminus A)$ contains no points of J i.e. if $\frac{s_i}{3} < |x_i| < \frac{2.5s_i}{3}$, then $|F_i(\lambda_1, x_i)| - 2s_i > 0$. Note that $|g| < \beta(1 + x^2)$. Assume $\frac{s_i}{3} < |x_i| < \frac{2.5s_i}{3}$, for $C(x_i) = s_i^2 x_i - x_i^3$. Then

$$\left|C\left(\frac{s_i}{3}\right)\right| = \frac{8s_i^3}{27} > \left|C\left(\frac{2.5s_i}{3}\right)\right| = \frac{6.875s_i^3}{27} ,$$

which implies that over the interval, $\min |C(x_i)| = \frac{6.875s_i^3}{27}$. Thus,

$$\begin{aligned} |F_i(\lambda_1, x_i)| - 2s_i &\geq \frac{6.875s_i^3}{27} - \beta\left(1 + \frac{6.25s_i^2}{9}\right) - 2s_i \\ &\geq .25s_i^3 - \beta - 2s_i \\ &= .25(K_i(\lambda_1))^{\frac{3}{2}} - .69\beta(K_i(\lambda_1)) - 2\sqrt{K_i(\lambda_1)} - \beta . \end{aligned}$$

This expression grows without bound as $\lambda_1 \to \infty$. Thus we can pick a λ_1 sufficiently large that $|F_i(\lambda_1, x_i)| - 2s_i > 0$ in this region. Therefore, $F(\lambda_1, x)$ is not in J.

3. Let $M = \sup_{i \in \{1,\ldots,N\}, \lambda < \lambda_1} K_i(\lambda)$. M is finite. We assume $M \geq 2$ (if not set $M = 2$). Let $B = [x||x_i| \leq (2M + 2\beta)^{\frac{2}{3}}; i = 1, 2, 3..., N]$, $\forall i$, $g_i(\lambda, x) \leq \beta$. For every $x \in \mathbb{R}^N \setminus B$ there exits i such that $|x_i| \geq (2M + 2\beta)^{\frac{2}{3}}$. Then

$$F_i(\lambda, x) - x_i = K_i(\lambda)x_i - x_i^3 + \beta - x_i .$$

Let $x_i = (2M + 2\beta)^{\frac{2}{3}}$. Then

$$\begin{aligned} F_i(\lambda, x) - x_i &= K_i(\lambda)x_i - x_i^3 + \beta - x_i \\ &\leq -x_i^3 + (M-1)x_i + \beta \\ &= -(2M+2\beta)^2 + (M-1)(2M+2\beta)^{\frac{2}{3}} + \beta \\ &= (2M+2\beta)^{\frac{2}{3}}[-(2M+2\beta)^{\frac{4}{3}} + (M-1)] + \beta \end{aligned}$$

$since - (2M + 2\beta) > -(2M + 2\beta)^{\frac{4}{3}}$

$$\begin{aligned} &\leq (2M+2\beta)^{\frac{2}{3}}[-(2M+2\beta) + (M-1)] + \beta \\ &= (2M+2\beta)^{\frac{2}{3}}[-2M - 2\beta + M - 1] + \beta \\ &= (2M+2\beta)^{\frac{2}{3}}[-M - 2\beta - 1] + \beta \\ &\leq (2M+2\beta)^{\frac{2}{3}}[-M - 2\beta - 1] + \beta(2M+2\beta)^{\frac{2}{3}} \\ &= (2M+2\beta)^{\frac{2}{3}}[-M - 2\beta - 1 + \beta] \\ &= (2M+2\beta)^{\frac{2}{3}}[-M - \beta - 1] \\ &= (2M+2\beta)^{\frac{2}{3}}[-(M+\beta) - 1] \\ &\leq -(M+\beta)\ . \end{aligned}$$

Since $M > 2$ and $\beta > 0$, the last inequality is true.

Let $G_i(x) = F_i(\lambda, x) - x_i = K_i(\lambda)x_i - x_i^3 + \beta - x_i$ and $x_i = -(2M + 2\beta)^{\frac{2}{3}}$.

Then

$$\begin{aligned} G_i(x) &= (2M+2\beta)^2 + (M-1)(-(2M+2\beta)^{\frac{2}{3}}) + \beta \\ &= (2M+2\beta)^{\frac{2}{3}}((2M+2\beta)^{\frac{4}{3}} - (M-1)) + \beta \\ &\geq (2M+2\beta)^{\frac{2}{3}} \end{aligned}$$

provided

$$\begin{aligned} (2M+2\beta)^{\frac{4}{3}} - M + 1 &\geq 1 \\ (2M+2\beta)^{\frac{4}{3}} - M &\geq 0 \\ (2M+2\beta)^{\frac{4}{3}} &\geq M \\ (2M+2\beta)^4 &\geq M^3 \, . \end{aligned}$$

which is true. Therefore, the ith component of the orbit is strictly monotonically decreasing by a positive amount, implying the trajectory is not bounded.

4. Fix A_j and λ_1 be large enough for (3) and (4) to hold. From (3) and (4) we know that image of $\mathbb{R}^N \setminus A_j$ lies strictly outside of J. F maps $J \setminus A$ to the left and right of J and $\mathbb{R}^N \setminus J$ to the right of J. Therefore, by Intermediate value theorem $F(\lambda_1, A_j) \cap J$ is non empty. Now we have to show $J \subset C$ where $C = F(\lambda_1, A_j)$ and F maps A_j diffeomorphically on J. In (3) and (4) we have shown that the image of the boundary of A_j does not intersect J. Since $D_x F$ is non singular on A_j, F is a local diffeomorphism on A_j. Therefore, the interior of A_j maps to an open set. The set C is compact, so each point of the boundary of C is the image of a boundary point of A_j. As shown above, there exists a point $z \in J \cap F(A_j)$. Let y be any point not in the compact set C. On the straight line segment from y to z, let w be the point closest to y that is in C. Then w is in the image of the boundary of A_j, so w is not in J. Since z is in the convex set J but w is not, y is not in J. Hence, no point outside of C is

in J. Hence, J is a subset of C.

□

This completes the proof of the five estimates. The result follows from these steps as follows: From the steps (2)-(5) it is shown that for large λ, on the invariant set in J, the family of N-coupled cubic maps is topologically conjugate to the full shift on 3^N symbols associated with 3^N rectangles A_i. Specifically all orbits are hyperbolic. From (4), it follows that there are no orbits near or on the boundary of J for all λ between λ_0 and λ_1. (2) shows that at λ_1, and any point in A, D_xF is diagonally dominant and the dynamics is expansive. Since G is topologically conjugate to the shift on 3^N symbols, with correspondence between the signs of the eigenvalues of the Jacobian of G and the signs of the eigenvalues of the Jacobian of F for large λ, each regular period k orbit for G is in one-to-one correspondence to a regular period k orbit for $F(\lambda_1, .)$, and each of these orbits is contained in a cascade component with stem period k. From (1) it follows that for N-odd, there is one flip fixed point P for $\lambda \to -\infty$. Every regular orbit for the shift map on 3^N symbols corresponds to an orbit of $F(\lambda_1, .)$. In other words, there are no regular regular orbits at λ_0 and infinitely many orbits at λ_1. This and steps (1)-(5) show that by Theorem 2.1.10 part C_0 all but possibly one of the regular orbits for $\lambda = \lambda_1$ are contained in a unique unbounded cascades components. For N-even, we have a regular fixed point for P for $\lambda \to -\infty$. This is the only regular (entry) orbit at $\lambda = \lambda_0$ and there are infinitely many orbits at λ_1. Therefore, in this case the result follows from Theorem 2.1.10 part C_K.

This completes the proof.

Let us consider the case of N-odd, because in this case we can count the cascades using the results of [21]. Since each map $T_3(x_i)$ in $G(X)$, has 2 negative symbols -1_L and -1_R corresponding to the left and the right sub-interval, and +1 corresponding to the central sub-interval. Therefore, $G(X)$ has 3^N symbols out of which $\frac{3^N-(-1)^N}{2}$ are negative and $\frac{3^N+(-1)^N}{2}$ are positive. Therefore, by Lemma 5 in [21], F has $\left[3^N, \frac{3^N+(-1)^N}{2}\right]$ dynamical horseshoe and therefore for a residual set of g for which F is generic, the number of stem period-k solitary cascades is given by $\rho_s\left[3^N, \frac{3^N+(-1)^N}{2}, k\right]$.

2.4 Counting Cascades of a mixed family of quadratic and cubic maps

In [21], Joglekar, Sander and Yorke proved the existence of cascades and also gave a way to enumerate the cascades as a function of the periodic orbits from which they arise. In particular they show that its sufficient to count the number of regular periodic orbits by proving that the number of regular periodic orbits is approximately half of the total number of periodic orbits. Thus, if there are infinitely many of one, there are infinitely many of the other. They give a recursive formula for the number of regular periodic orbits of an m-shift. They define a mapping Sgn with range ± 1 on the m fixed points. If Sgn is positive on the fixed point $(s, s, s, ...)$ it is referred to as a positive symbol and a negative symbol if Sgn is negative. If there are j positive symbols and $(m - j)$ negative symbols the shift mapping is denoted as $\sigma_{(m,j)}$. The mapping Sgn can be extended to periodic orbits as: Let $(s_1, s_2, ...)$ be a periodic point under $\sigma_{(m,j)}$, let r be the number of symbols in the set $(s_1, s_2, ...s_k)$ (with multiplicity) which are negative, then $Sgn(s, k) = (-1)^r$. Let $a = (a_1, a_2, ...)$ be a least period-k point of the shift map $\sigma_{(m,j)}$. The point a is called a regular periodic point if $Sgn(s, k) = 1$. Define $\rho_s(m, j, k) =$ the set of regular period-k points of $\sigma_{(m,j)}$, $e(m, j, k) =$ the set of fixed points of $\sigma^k_{(m,j)}$ such that $Sgn(., k) = 1$.

Theorem 2.4.1. *(Main result of [21]) Recursive counting formula for RPOs of an m-shift. Let*

$$Odd(k) = [n < k; k/n \text{ is odd}]$$

If k is odd, then

$$|\rho_s(m, j, k)| = |e(m, j, k)| - \sum_{n \in Odd(k)} |\rho_s(m, j, n)|$$

and if k is even, then

$$|\rho_s(m, j, k)| = |e(m, j, k)| - \sum_{n \in Odd(k)} |\rho_s(m, j, n)| - m^{k/2}$$

where $|.|$ denotes the number of elements in the set.

To compute $|e(m, j, k)|$ the following lemma is used.

Lemma 2.4.2. *Assume that*

$$j = \frac{m + l}{2}$$

This is equivalent to $j - (m - j) = l$, meaning that l is the difference between the number of the positive and the number of negative symbols. The quantity l can be either positive or negative. Then,

$$|e(m, j, k)| = \frac{m^k + l^k}{2}.$$

In this section, we use this result to prove that a mixed family of cubic and quadratic maps has infinitely many cascades and we also give the number of cascades for each period-k. Consider a mixed family of quadratic and cubic maps defined as: Let $G : \mathbb{R}\times\mathbb{R}^N \to \mathbb{R}^N$ and $g : \mathbb{R}\times\mathbb{R}^N \to \mathbb{R}^N$ be smooth and let each component G_i have the form

$$G_i(\lambda, x_1, x_2, \ldots, x_N) = F_i(\lambda, x_i) + g_i(\lambda, x_1, x_2, \ldots, x_N)$$

for each $i = 1, 2, 3..., N$, where F_i is $\lambda - x_i^2$ or $\lambda x_i - x_i^3$ and g is such that for some $\beta > 0$, $||g(\lambda, 0)|| < \beta$ and $||D_x g(\lambda, x)|| < \beta$.

Out of the N maps, let p be the number of quadratic maps ($\lambda - x^2 + g(\lambda, x)$) and q be the number of cubic maps ($\lambda x - x^3 + g(\lambda, x)$), then we can use the results of [21] to count the number of cascades by counting the number of positive and negative symbols. In particular for a mixed family of maps, with at least one of the maps being a quadratic map, the following result is true.

Lemma 2.4.3. *The number of positive and negative symbols for a mixed family of N-coupled maps is independent of the order in which the cubic and the quadratic maps are arranged. Furthermore the number of positive and negative symbols is the same and equal half of the total number of symbols.*

Proof of lemma: Suppose we have a map $g(\lambda, x)$, and we know the number of positive and negative symbols of g. Let m and n be the number of positive and negative symbols of g. Consider the map

$$F = \begin{pmatrix} g \\ Q \end{pmatrix}$$

where Q is the quadratic map $\lambda - x^2$. Since the quadratic map has 1 positive and 1 negative symbol, the total number of symbols for F is $2(m+n)$. The number of positive symbols of F is given by m times the number of positive symbols of Q, and n times the number of negative symbols of Q, therefore the number of positive symbols is $m+n$. By a similar reasoning the number of negative symbols is also $m+n$. Therefore, the number of positive and negative symbols is half of the total number of symbols. The coupling function g does not affect the number of positive and negative symbols as is evident from the following argument.

It has been proved in [47] for a family of coupled quadratic maps given by

$$F_i(\lambda, x_1, x_2, \ldots, x_N) = K_i(\lambda) + g_i(\lambda, x_1, x_2, \ldots, x_N)$$

for each $i = 1, 2, 3..., N$, where g is such that for some $\beta > 0$, $||g(\lambda, 0)|| < \beta$ and $||D_x g(\lambda, x)|| < \beta$, for a sufficiently large value of λ the maximal bounded invariant set is conjugate to the shift map on 2^N symbols. It is also shown in the proof that on this set and for this value of λ, F is diagonally dominant and the map is expansive. $D_x F$ for this family is given by

$$D_x F = \begin{bmatrix} K_1(\lambda_1) - 2x_1 + \frac{\partial g_1}{\partial x_1} & \frac{\partial g_1}{\partial x_2} & \ldots & \frac{\partial g_1}{\partial x_N} \\ \vdots & \vdots & \ddots & \vdots \\ \frac{\partial g_N}{\partial x_1} & \frac{\partial g_N}{\partial x_2} & \ldots & K_N(\lambda_1) - 2x_N + \frac{\partial g_N}{\partial x_N} \end{bmatrix}$$

Since the partial derivatives of g are bounded, this implies that the diagonal entries grow arbitrarily large as we increase λ_1. Hence the $D_x F$ is diagonally dominant and the map is expansive on this

Table 2.1: The number of regular period-k orbits for the mixed family of maps. (Q,C) represents the number of quadratic and cubic maps in the family.

(Q,C)	(m, j)	$k = 1$	$k = 2$	$k = 3$	$k = 4$	$k = 5$
(1,1)	(6,3)	3	6	35	153	777
(1,2)	(18,9)	9	72	969	13041	188955
(2,1)	(12,6)	6	30	286	2556	24882
(2,2)	(36,18)	18	306	7770	209628	6046614
(1,3)	(54,27)	27	702	26235	1062153	45916497
(3,1)	(24,12)	12	132	2300	41328	796260
(2,3)	(108,54)	54	2862	209934	17003196	1469328066
(3,2)	(72,36)	36	1260	62196	3357936	193491756
(3,3)	(216,108)	108	11556	1679580	272086128	47018498436

set. Using a similar argument we proved in this paper that the maximal bounded invariant set for a coupled family of cubic maps is conjugate to a shift map on 3^N symbols and that the dynamics is expansive. Since for a period-k point,

$$D_x[f^k(x_1)] = D_x f[x_{k-1}] D_x f[x_{k-2}] ... D_x f[x_0]$$

therefore, sign of a periodic orbit depends only on the product of the diagonal entries. And since the sign of a period-k point is determined by the product of the signs of the eigenvalues of the Jacobian at each point in the periodic orbit, the order in which the maps are arranged does not matter. Hence we can use the results of [21] to count the number of cascades of these maps. The number of period-k cascades are counted by counting the number of regular periodic points for each period k, given by $|\rho_s(m, j, k)|$ where m is the total number of symbols, j is the number of positive symbols. The Table 2.1 gives the number of cascades of each period-k for $k = 1$ to 5 for the mixed family of maps. These values are calculated using the Mathematica program given in [21]. Even though Mathematica is used to implement the counting algorithm, note that these are based on analytical results.

2.5 5- and 6-horseshoes

So far our examples have been limited to coupling of quadratic and cubic maps. In fact, we can couple any k-horseshoes and get similar results. For example in the introduction, we mentioned an example of a quartic map that transitions from order to a 4-horseshoe. Keep in mind that not all families of quadratic, cubic, or quartic maps satisfy the requirements to be a k-map. In this section we give examples of k-maps for $k = 5, 6$. That is, they have the property that they exhibit infinite number of period-doubling cascades, for each j, the number of period-j cascades can be enumerated, and these cascades are preserved even under large additive perturbations. These maps have been carefully derived to satisfy the property that for large values of the parameter it forms a horseshoe. The equations have been chosen so that the stretching in the vertical direction is faster than the stretching in the horizontal direction as the parameter increases. These maps can be coupled with any of the previously discussed quadratic, cubic, and quartic maps to give additional cases of N-dimensional coupled systems with period-doubling cascades. In Figure 2.3, the overlap of periodic orbits and the attracting set for the quintic map is depicted without a perturbation and with a perturbation.

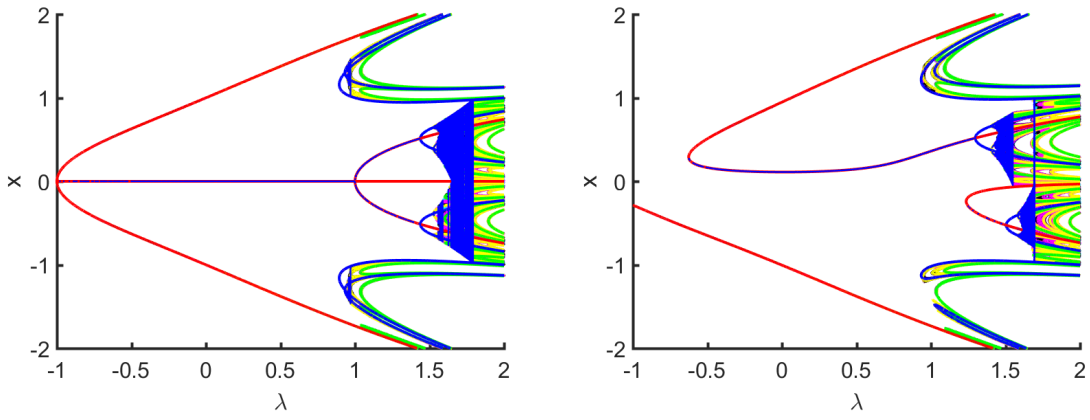

Figure 2.3: In the left picture periodic orbits (periods 1 through 8) are shown overlapped with the bifurcation diagram of $f(\lambda, x) = \lambda^2 x - 3\lambda x^3 + x^5$ and the right picture shows the periodic orbits (periods 1 through 8) overlapped with the bifurcation diagram for $F(\lambda, x) = \lambda^2 x - 3\lambda x^3 + x^5 + 0.7 \sin x + 0.7$.

Theorem 2.5.1. *Consider the parametrized degree 5 polynomial*

$$quint(\lambda, x) = \lambda^2 x - 3\lambda x^3 + x^5 + g(\lambda, x),$$

where $g : \mathbb{R} \times \mathbb{R} \to \mathbb{R}$ *is* C^∞ *such that for some* $\beta > 0$, $|g(\lambda, 0)| < \beta$ *and for all* λ *and* x, $|\frac{\partial g}{\partial x}(\lambda, x)| < \beta$. *The quint map is a* 5*-map.*

Proof. We will show that there exists an interval $[\lambda_1, \lambda_2]$, such that for λ_1 sufficiently negative there are no or finite number of regular periodic orbits and for λ_2 sufficiently large there is a one dimensional horseshoe. Let $F(\lambda, x) = \lambda^2 x - 3\lambda x^3 + x^5$. The conditions on g guarantee that for sufficiently large values of $|\lambda|$, g does not significantly affect the periodic orbits of F. Hence, the number of period-k cascades of perturbed map $F + g$ is same as F. Proof is divided into the following steps.

(i) For λ sufficiently negative, $F(\lambda, x)$ has only one fixed point $x = 0$ and for $\lambda < -1$ it is a unstable fixed point.

$$F(\lambda, x) - x \quad = \quad x^5 - 3\lambda x^3 + x(\lambda^2 - 1)$$

Solving $F(\lambda, x) - x = 0$ gives $x = 0$ and $x = \pm\sqrt{\frac{3\lambda \pm \sqrt{5\lambda^2+1}}{2}}$. From the above expression we can see that for $\lambda < -1$, $x = 0$ is the only fixed point and no other periodic points exist. For $\lambda < -1$, $F'(\lambda, x) > 0$ for all x. Therefore $F(\lambda, x)$ is increasing. Since $\lim_{x\to\infty} F(\lambda, x) \to \infty$ and $\lim_{x\to-\infty} F(\lambda, x) \to -\infty$, and $F(\lambda, x)$ is above the diagonal for $x > 0$ and below the diagonal for $x < 0$, therefore are no other periodic orbits.

(ii) For λ sufficiently negative and g of the above form, let $h(\lambda, x) = F(\lambda, x) + g(\lambda, x)$. Need to

show $|\frac{\partial h(\lambda,x)}{\partial x}| > 1$ for all x.

$$\begin{aligned} \left|\frac{\partial h}{\partial x}\right| &\geq |F'(\lambda,x)| - |g'(\lambda,x)| \\ &> 5x^4 - 9\lambda x^2 + \lambda^2 - \beta \end{aligned}$$

This last expression is positive as long as $\lambda < -\sqrt{\beta}$. Therefore, $F(\lambda,x) + g(\lambda,x)$ is an increasing function. Since $\lim_{x\to\infty}(F(\lambda,x) + g(\lambda,x)) \to \infty$ and $\lim_{x\to-\infty}(F(\lambda,x) + g(\lambda,x)) \to -\infty$, and $F(\lambda,x) + g(\lambda,x)$ is above the diagonal for $x > 0$ and below the diagonal for $x < 0$, therefore there is a unique fixed point.

(iii) For λ positive and sufficiently large, we will show that there is a one dimensional horseshoe.
(i)For λ sufficiently large, there exists a λ-dependent box which contains all the periodic orbits.

$F(\lambda,x)$, under the following scaling can be written as $F(\lambda,\sqrt{\lambda}x) = \lambda^{5/2}(x^5 - 3x^3 + x) = \lambda^{5/2}f(x)$, where $f(x) = x^5 - 3x^3 + x$. We show that the results are true for $f(x)$ as the calculations are much simpler and then we will prove they are true for $F(\lambda,x)$. $f(x)$ has two local minima $\{(-0.34,-0.23),(1.3,-1.58)\}$ and two local maxima $\{(0.34,0.23),(-1.3,1.58)\}$. Therefore, $F(\lambda,x)$ has two local minima $\{(-0.34\sqrt{\lambda},-0.23\lambda^{5/2}),(1.3\sqrt{\lambda},-1.58\lambda^{5/2})\}$ and two local maxima $\{(0.34\sqrt{\lambda},0.23\lambda^{5/2}),(-1.3\sqrt{\lambda},1.58\lambda^{5/2})\}$. Therefore, as $\lambda \to \infty$, $F(\lambda,x)$ is stretched in the horizontal direction by a factor of $\sqrt{\lambda}$ and in the vertical direction by a factor of $\lambda^{5/2}$. See Figure 2.4.

All the periodic orbits of F lie in the interval $I = \left[-2\sqrt{\lambda}, 2\sqrt{\lambda}\right]$. Since $F(\lambda,x) = \lambda^{5/2}f(\frac{x}{\sqrt{\lambda}})$. Consider the case for $\lambda = 4$. We will show that all periodic orbits of $f(x)$ are contained in the interval $[-4,4]$.

$$\begin{aligned} f(x) - x &= (x^5 - 12x^3 + 16x) - x \\ &= x^5 - 12x^3 + 15x \end{aligned}$$

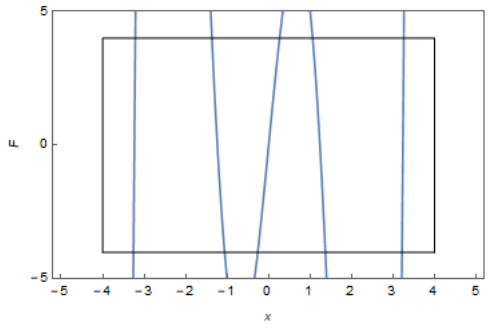

Figure 2.4: In this picture $F(\lambda, x)$is shown for $\lambda = 4$ and the square depicted is $\left[-2\sqrt{\lambda}, 2\sqrt{\lambda}\right]^2$. As λ increases, the values at the maxima and minima grow at a rate proportional to $\lambda^{5/2}$ and become larger than the size of the box resulting in the creation of a horseshoe.

Solving $f(x) - x = 0$ gives five fixed points $x = 0, \pm 1.19, \pm 3.25$, all of which lie inside the interval $[-4, 4]$. Also for $x > 4$, $f(x) - x > 0$ and for $x < -4$, $f(x) - x < 0$, therefore there are no periodic orbits outside $[-4, 4]$. Because $F(\lambda, x) = \lambda^{5/2} f(\frac{x}{\sqrt{\lambda}})$, therefore for λ sufficiently large, the fixed points of $F(\lambda, x)$ are given by $\frac{x}{2}\sqrt{\lambda}$ and therefore lie inside $\left[-2\sqrt{\lambda}, 2\sqrt{\lambda}\right]$. For $x > 2\sqrt{\lambda}$,

$$\begin{aligned} F(\lambda, x) - x &= x^5 - 3\lambda x^3 + \lambda^2 x - x \\ &= x^5 - 3\lambda x^3 + x(\lambda^2 - 1) \\ &> 10\lambda^{5/2} - 2\sqrt{\lambda} \end{aligned}$$

This quantity grows arbitrary large as $\lambda \to \infty$. Therefore as long as $10\lambda^{5/2} - 2\sqrt{\lambda} > 0$, $F(\lambda, x)$ is above the diagonal. A similar calculation shows that this is true for $x < -2\sqrt{\lambda}$.

(ii) $\left|\frac{\partial F(\lambda,x)}{\partial x}\right|$ is greater than 1 inside the box. Consider the case when $\lambda = 4$. $F(4, x) = x^5 - 12x^3 + 16x$. Inside $[-4, 4]$, $|F'(4, x)| > 1$ on the following five intervals. $A_1 = [-4, -2.6]$, $A_2 = [-2.59, -0.71]$, $A_3 = [-0.67, 0.67]$, $A_4 = [0.71, 2.59]$, $A_5 = [2.6, 4]$

and the function maps across the entire interval. Since $F(\lambda, x) = \lambda^{5/2} f\left(\frac{x}{\sqrt{\lambda}}\right)$, $F'(\lambda, x) = \lambda^2 f'\left(\frac{x}{\sqrt{\lambda}}\right)$. Therefore, $|F'(\lambda, x)| = \lambda^2 |f'\left(\frac{x}{\sqrt{\lambda}}\right)| > 1$ on the following intervals, $A_1 = [-2s, -1.3s]$, $A_2 = [-1.295s, -0.36s]$, $A_3 = [-0.34s, 0.34s]$, $A_4 = [0.36s, 1.295s]$, $A_5 = [1.3s, 2s]$ where $s = \sqrt{\lambda}$ and the function maps across $\left[-2\sqrt{\lambda}, 2\sqrt{\lambda}\right]$ five times creating a horseshoe.

(iv) Now we show that the above is true with g added. Let $h(\lambda, x) = F(\lambda, x) + g(\lambda, x)$. For lambda sufficiently large, there are no periodic orbits outside of $\left[-2\sqrt{\lambda}, 2\sqrt{\lambda}\right]$. The conditions on $g(\lambda, x)$ guarantee that $|g(\lambda, x) < \beta + \beta|x|$. Let $x > 2\sqrt{\lambda}$.

$$\begin{aligned} h(\lambda, x) - x &= x^5 - 3\lambda x^3 + \lambda^2 x + g(\lambda, x) - x \\ &> 10\lambda^{5/2} - 2\sqrt{\lambda} - \beta - \beta|x| \\ &> 10\lambda^{5/2} - 2\sqrt{\lambda}(1 + \beta) - \beta \end{aligned}$$

This last quantity grows arbitrary large as $\lambda \to \infty$. Therefore as long as $10\lambda^{5/2} - 2\sqrt{\lambda}(1 + \beta) - \beta > 0$, $h(\lambda, x)$ is above the diagonal for $x > 2\sqrt{\lambda}$. A similar calculation shows that $h(\lambda, x)$ is below the diagonal for $x < -2\sqrt{\lambda}$. Therefore there are no periodic orbits outside $\left[-2\sqrt{\lambda}, 2\sqrt{\lambda}\right]$.

Next to show $\left|\frac{\partial h(\lambda, x)}{\partial x}\right|$ is greater than 1 inside the box.

$$\begin{aligned} \left|\frac{\partial h(\lambda, x)}{\partial x}\right| &> \left|\frac{\partial F(\lambda, x)}{\partial x}\right| - \left|\frac{\partial g(\lambda, x)}{\partial x}\right| \\ &> \lambda^2 \left|f'\left(\frac{x}{\sqrt{\lambda}}\right)\right| - \beta \end{aligned}$$

Therefore, as long as $\lambda > \sqrt{\frac{\beta+1}{\left|f'\left(\frac{x}{\sqrt{\lambda}}\right)\right|}}$, $\left|\frac{\partial h(\lambda,x)}{\partial x}\right| > 1$ on the intervals $A_1, A_2, A_3, A_4,$ and A_5 defined in part (iii).

Hence, we can find an interval, $[\lambda_1, \lambda_2]$ for $quint(\lambda, x)$ such that there are no regular periodic orbits for λ_1 sufficiently negative and for λ_2 sufficiently large there is a one dimensional horseshoe, which implies there are infinitely many period doubling cascades. This completes the proof.

Using the enumeration results from [21], we can give the number of finite period-k cascades for the $quint$ map. The table below shows the values for $k = 1$ to $k = 7$.

Table 2.2: The number of regular period-k orbits for the $quint$ family of maps.

(m, j)	$k = 1$	$k = 2$	$k = 3$	$k = 4$	$k = 5$	$k = 6$	$k = 7$
(5,3)	3	4	20	72	312	1280	5580

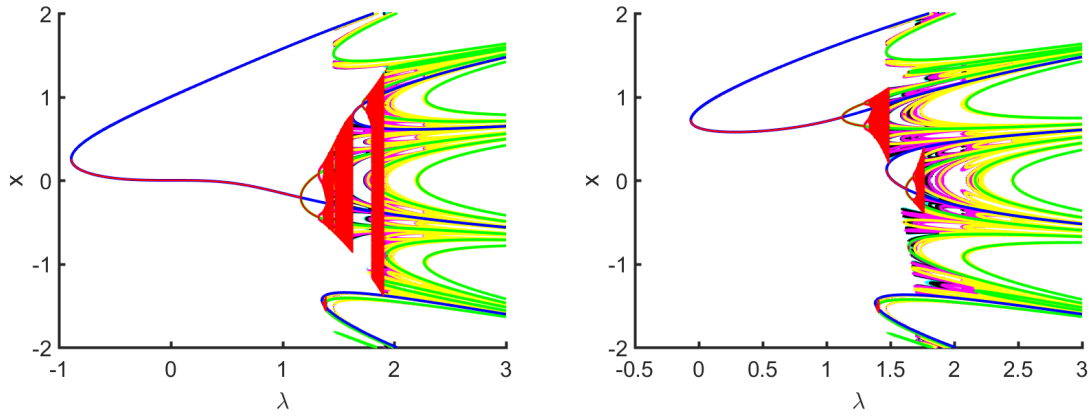

Figure 2.5: Left picture shows the periodic orbits (periods 1 through 4) overlapped with the bifurcation diagram for the map $f(\lambda, x) = x^6 - 3\lambda x^4 + 2\lambda^2 x^2 - \frac{\lambda^3}{5}$, and the right picture shows the overlap for the map $hex(x) = x^6 - 3\lambda x^4 + 2\lambda^2 x^2 - \frac{\lambda^3}{5} + 0.7\cos x$

Theorem 2.5.2. *Consider the degree 6 polynomial*

$$hex(x) = x^6 - 3\lambda x^4 + 2\lambda^2 x^2 - \frac{\lambda^3}{5} + g(\lambda, x),$$

with the same conditions on g as in the case of degree 5 polynomial. Then hex is a 6-map.

Proof. We show the existence of λ sufficiently small for which there are no regular periodic points and λ sufficiently large for which there exists a one dimensional horseshoe. In Figure 2.5, the overlap of periodic orbits and the attracting set for the hex map is depicted without a perturbation and with a perturbation.

Let $F(\lambda, x) = x^6 - 3\lambda x^4 + 2\lambda^2 x^2 - \frac{\lambda^3}{5}$. The conditions on g guarantee that for sufficiently large values of $|\lambda|$, it does not significantly affect the periodic orbits of F. Hence, the number of period-k cascades of perturbed map $F + g$ is same as F. Proof is divided into the following steps.

(i) For λ sufficiently negative,we show that there are no periodic orbits. Let $M(\lambda, x) = F(\lambda, x) - x = x^6 - 3\lambda x^4 + 2\lambda^2 x^2 - \frac{\lambda^3}{3} - x$. We will prove that for λ sufficiently negative $M(\lambda, x) > 0$. $M'(\lambda, x) = 6x^5 - 12\lambda x^3 + 4\lambda^2 x - 1$. Since $M'(\lambda, 0) = -1$ and $M'(\lambda, 1) = 4\lambda^2 - 12\lambda + 5 > 0$ for $\lambda < 0$, therefore there exists a point c close to zero such that $M'(\lambda, c) = 0$. Also for $x < c$, $M'(\lambda, x) < 0$ and for $x > c$, $M'(\lambda, x) > 0$ which implies that $x = c$ is a minimum point for $M(\lambda, x)$ and $M(\lambda, c) > 0$. Therefore, for λ large and negative, $F(\lambda, x) - x > 0$ and hence there are no periodic orbits.

(ii) Let $h(\lambda, x) = x^6 - 3\lambda x^4 + 2\lambda^2 x^2 - \frac{\lambda^3}{5} + g(\lambda, x)$ where for $\beta > 0$, $g(\lambda, x)$ satisfies $|g(\lambda, 0)| < \beta$ and $\left|\frac{\partial g}{\partial x}\right| < \beta$. We will prove that for λ sufficiently negative and $\lambda < -1$, $h(\lambda, x) > x$ and hence there are no periodic orbits.

$$\begin{aligned} h'(\lambda, x) &= F'(\lambda, x) + g'(\lambda, x) \\ &= 6x^5 - 12\lambda x^3 + 4\lambda^2 x + g'(\lambda, x) \end{aligned}$$

From the above expression it is easy to see that for $x < 0$ and for $\lambda < -1$ $F'(\lambda, x) < 0$ and for $x > 0$ and $\lambda < -1$, $F'(\lambda, x) > 0$. Since $\left|\frac{\partial g}{\partial x}\right| < \beta$, we can choose λ sufficiently negative such that $h'(\lambda, x) < 0$ for $x < 0$ and $h'(\lambda, x) > 0$ for $x > 0$. Also

$$\begin{aligned} h(\lambda, 0) &= -\frac{\lambda^3}{5} + g(\lambda, 0) \\ &> -\frac{\lambda^3}{5} - \beta \end{aligned}$$

Therefore as long as $\lambda < (-5\beta)^{1/3}$, $h(\lambda, 0) > 0$. Hence, we can choose λ sufficiently negative so that there is a point close to zero which is a minimum point for $h(\lambda, x)$ such that $h(\lambda, 0) > 0$. Also since $\lim_{x\to\infty} h(\lambda, x) \to \infty$ and $\lim_{x\to-\infty} h(\lambda, x) \to \infty$, therefore $h(\lambda, x) > x$ and there are no periodic orbits.

(iii) Instead of working with $F(\lambda, x)$, we work with a scaled version of this function. Consider $F(\lambda, \sqrt{\lambda}x) = \lambda^3(x^6 - 3x^4 + 2x^2 - 1/5) = \lambda^3 f(x)$. Assume $\lambda > 0$. $F(\lambda, x)$ has the same properties as $f(\lambda, x)$ but the calculations are much simpler with the latter function. $f(x)$ has 3 local minima $(0, -0.2), (-1.26, -0.58), (1.26, -0.58)$ and 2 local maxima $(-0.65, 0.18), (0.65, 0.18)$. Therefore, $F(\lambda, x)$ also has 3 local minima and 2 local maxima and the values at these critical points are the values of $f(x)$ multiplied by a factor of λ^3. Therefore, as $\lambda \to \infty$, the map is stretched in the vertical direction and the values at the peaks grow at a rate proportional to λ^3. See Figure 2.6.

All the periodic orbits of F lie in the interval $I = \left[-2\sqrt{\lambda}, 2\sqrt{\lambda}\right]$. Since $F(\lambda, x) = \lambda^{5/2} f(\frac{x}{\sqrt{\lambda}})$. Consider the case for $\lambda = 3$. We will show that all periodic orbits of $f(x)$

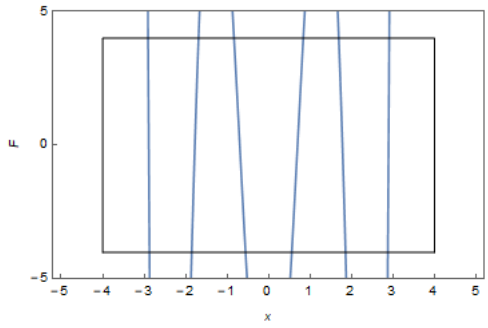

Figure 2.6: In this figure $F(\lambda, x)$ and the box $\left[-2\sqrt{\lambda}, 2\sqrt{\lambda}\right]^2$ has been drawn for $\lambda = 4$. As λ increases the maxima and minima grow at a rate proportional to λ^3 and the values are larger than the size of the box.

are contained in the interval $\left[-2\sqrt{3}, 2\sqrt{3}\right]$.

$$\begin{aligned} f(x) - x &= (x^6 - 9x^4 + 18x^2 - \frac{27}{5}) - x \\ &= x^6 - 9x^4 + 18x^2 - x - \frac{27}{5} \end{aligned}$$

Solving $f(x) - x = 0$ gives 6 fixed points $x = -2.48, -1.60, -0.56, 0.65, 1.47, 2.52$, all of which lie inside the interval $\left[-2\sqrt{3}, 2\sqrt{3}\right]$. Also for $|x| > 2\sqrt{3}$, $f(x) - x > 0$ and it is increasing, therefore there are no periodic orbits outside $\left[-2\sqrt{3}, 2\sqrt{3}\right]$. Because $F(\lambda, x) = \lambda^{5/2} f(\frac{x}{\sqrt{\lambda}})$, therefore for λ sufficiently large, the fixed points of $F(\lambda, x)$ are given by $\frac{x}{\sqrt{3}}\sqrt{\lambda}$ and therefore lie inside $\left[-2\sqrt{\lambda}, 2\sqrt{\lambda}\right]$. For $x > 2\sqrt{\lambda}$,

$$\begin{aligned} F(\lambda, x) - x &= x^6 - 3\lambda x^4 + 2\lambda^2 x^2 - \frac{\lambda^3}{5} - x \\ &> \frac{119}{5}\lambda^3 - 2\lambda^{1/2} \end{aligned}$$

This quantity grows arbitrary large as $\lambda \to \infty$. Therefore as long as $\frac{119}{5}\lambda^3 - 2\lambda^{1/2} > 0$, $F(\lambda, x)$ is above the diagonal. A similar calculation shows that this is true for $x < -2\sqrt{\lambda}$. Therefore, all periodic orbits lie inside the box $\left[-2\sqrt{\lambda}, 2\sqrt{\lambda}\right]$.

$\left|\frac{\partial F(\lambda,x)}{\partial x}\right|$ is greater than 1 inside the box. Consider the case when $\lambda = 3$. $F(3,x) = 6x^5 - 36x^3 + 36x$. Inside $\left[-2\sqrt{3}, 2\sqrt{3}\right]$, $|F'(3,x)| > 1$ on the following six intervals. $A_1 = \left[-2\sqrt{3}, -2.18\right], A_2 = [-2.17, -1.14], A_3 = [-1.11, -0.03], A_4 = [0.03, 1.11], A_5 = [1.14, 2.17], A_6 = \left[2.18, 2\sqrt{3}\right]$ and the function maps across the entire interval six times. Since $F(\lambda, x) = \lambda^3 f\left(\frac{x}{\sqrt{\lambda}}\right)$, $F'(\lambda, x) = \lambda^{5/2} f'\left(\frac{x}{\sqrt{\lambda}}\right)$. Therefore, by a similar argument as in the case of *quint* map, $|F'(\lambda, x)| = \lambda^{5/2}|f'\left(\frac{x}{\sqrt{\lambda}}\right)| > 1$ on six intervals inside $\left[-2\sqrt{\lambda}, 2\sqrt{\lambda}\right]$ for all $\lambda > 3$. The function maps across six times creating a horseshoe.

(iv) Let $h(\lambda, x) = F(\lambda, x) + g(\lambda, x)$. For lambda sufficiently large, there are no periodic orbits outside of $\left[-2\sqrt{\lambda}, 2\sqrt{\lambda}\right]$. The conditions on $g(\lambda, x)$ guarantee that $|g(\lambda, x) < \beta + \beta|x|$. Let $x > 2\sqrt{\lambda}$.

$$\begin{aligned} h(\lambda, x) - x &= x^6 - 3\lambda x^4 + 2\lambda^2 x^2 - \frac{\lambda^3}{5} + g(\lambda, x) - x \\ &> \frac{119\lambda^3}{5} - 2\sqrt{\lambda}(1+\beta) - \beta \end{aligned}$$

This last quantity grows arbitrary large as $\lambda \to \infty$. Therefore as long as $\frac{119\lambda^3}{5} - 2\sqrt{\lambda}(1 + \beta) - \beta$, $h(\lambda, x)$ is above the diagonal for $x > 2\sqrt{\lambda}$. A similar calculation shows that $h(\lambda, x)$ is below the diagonal for $x < -2\sqrt{\lambda}$. Therefore there are no periodic orbits outside $\left[-2\sqrt{\lambda}, 2\sqrt{\lambda}\right]$.

Next to show $\left|\frac{\partial h(\lambda,x)}{\partial x}\right|$ is greater than 1 inside the box.

$$\begin{aligned}\left|\frac{\partial h(\lambda,x)}{\partial x}\right| &> \left|\frac{\partial F(\lambda,x)}{\partial x}\right| - \left|\frac{\partial g(\lambda,x)}{\partial x}\right| \\ &> \lambda^{5/2}\left|f'\left(\frac{x}{\sqrt{\lambda}}\right)\right| - \beta\end{aligned}$$

Therefore, as long as $\lambda > \sqrt[5]{\left(\frac{\beta+1}{\left|f'\left(\frac{x}{\sqrt{\lambda}}\right)\right|}\right)^2}$, $\left|\frac{\partial h(\lambda,x)}{\partial x}\right| > 1$ on the intervals $A_1, A_2, A_3, A_4, A-5,$ and A_6 defined in part (iii).

Hence, we can find an interval, $[\lambda_1, \lambda_2]$ for $hex(\lambda, x)$ such that there are no regular periodic orbits for λ_1 sufficiently negative and for λ_2 sufficiently large there is a one dimensional horseshoe, which implies there are infinitely many period doubling cascades. This completes the proof.

Using the enumeration results from [21], we can give the number of finite period-k cascades for the hex map. The table below shows the values for $k = 1$ to $k = 7$.

Table 2.3: The number of regular period-k orbits for the hex family of maps.

(m, j)	$k = 1$	$k = 2$	$k = 3$	$k = 4$	$k = 5$	$k = 6$	$k = 7$
(6,3)	3	6	35	153	777	3850	19995

2.6 Concluding remarks

In this chapter we have proved that if we couple N one dimensional k-maps which have the property that for a sufficiently small parameter value, there is only non-chaotic behavior with a finite number

of periodic orbits, and for a sufficiently large parameter value, there is dynamics which is topologically conjugate to a full shift on k symbols, then the period doubling cascades are preserved. k does not necessarily have to be the same for each map. This extends the results of Sander and Yorke [47]. We apply this result to the cases of $3, 5$ and 6-maps. We have also used the enumeration scheme developed in [21] to count the number of period-k cascades in each of the above cases and also for a coupled family of cubic and quadratic maps.

The results from this chapter will be used in the Chapter 3 where we consider two parameter families of maps with infinitely many cascades. In particular, we will use the results to connect the period doubling cascades observed when a single parameter is varied to the bifurcation diagrams drawn when both parameters are varied simultaneously. This kind of bifurcation diagram is drawn entirely in the parameter space and shrimp like structures are observed.

Chapter 3: Period doubling cascades in two parameter maps

3.1 Introduction

The bifurcation diagrams in Chapter 2 have been drawn by varying one parameter at a time. But more complex dynamical behavior is observed in two parameter families of maps with period doubling cascades if both parameters are varied simultaneously. Specifically, regions with non chaotic periodic orbits containing period doubling cascades have boundaries with many cusps. These structures resemble shrimps with many legs. See Figure 3.1. Shrimps can be seen as two parameter counterparts of cascades emanating from periodic windows. In this chapter we give a more precise definition of a shrimp and give results based on Chapter 2.

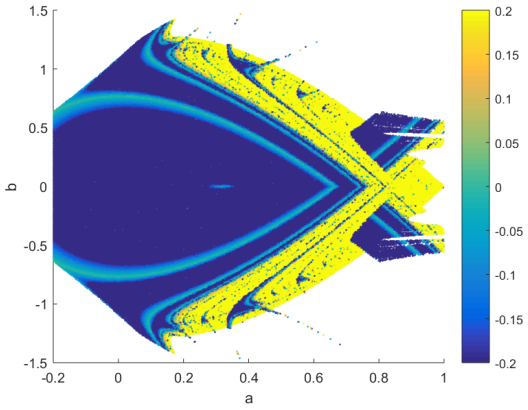

Figure 3.1: This is the Lyapunov graph for the cubic map $f(x) = -x^3 + 3ax - b$ where a and b are parameters. The color is the Lyapunov exponent. Therefore, the positive values (more yellow) corresponds to chaos, and the negative values (more blue) corresponds to regular behavior. The white space is the parameter values for which there is no stable behavior. This color scheme is used for all the figures in this Chapter. We have used the initial condition $x_0 = 0$ and the parameter values are chosen randomly from a grid of values. In this chapter, we are concerned with shrimp: in this figure these are the blue objects with four legs. This is described in Section 3.4

Shrimps have been previously observed by a variety of authors. For example, in [20], Hunt et al, discuss the structure of parameter space for two-parameter families of maps. Since there are two parameters, a bifurcation diagram is drawn entirely in the parameter space, instead of a bifurcation diagram with the phase space variable on one axis and the parameter on the other. There are a variety of tests for the dynamics of orbits at each fixed parameter pair. For example, in Figure 3.1, we have assigned color to the regions according to the computed Lyapunov exponent of the stable orbit. A common shape of the region with stable non-chaotic dynamics has been observed, called a swallow or a shrimp. The shrimp shape for the cubic map was first discussed by Milnor in [31] and then by Gallas in [16,17]. Shrimps have also been observed in the Henon map [15]. Since then shrimps have been observed in the parameter space of higher dimensional systems as well. See [1], [18], [52]. Milnor and others have pointed out the close relationship between shrimps and Arnold tongues. In [10], the authors have found shrimps in the Duffing oscillator and have pointed out as others the closeness of Arnold tongues to shrimps. We will not be exploring this relationship. Milnor states that for the cubic map, the swallow configuration is seen if we can find disjoint intervals around each critical point so that the first return map from the union of these intervals to itself is defined and smooth and interchanges these two components. The idea is that around each critical point the first return map can be approximated by a map that is quadratic.

In [52], Gallas and others have proposed the following definition of shrimps: "Shrimps are formed by a regular set of adjacent windows centered around the main pair of intersecting superstable parabolic arcs. A shrimp is a doubly infinite mosaic of stability domains composed by an innermost main domain plus all the adjacent domains arising from two period doubling cascades together with their corresponding domains of chaos." In contrast to this definition, in [12] a shrimp is described as a region in the parameter space bounded by period doubling bifurcation on one side and saddle node bifurcation on the other side. Specifically this definition implies that the region contains only periodic orbits of a single period, as opposed to an entire period doubling cascade. As should be clear that there are various definitions of a shrimp and many of these are not rigorous. There is no general agreement between them and no attempt has been made to compare them. In the next section, we give a series of definitions all of which have been used to describe a shrimp and give a

detailed comparison of these definitions, and give a scope for when these definitions do not agree.

3.2 Analysis of Shrimps

In this section, we consider families of two parameter smooth maps, $f(\lambda, x) : \mathbb{R} \times \mathcal{M} \to \mathcal{M}$, where $\mathcal{M}$ is a smooth n-dimensional space and $\lambda \in \mathbb{R}^2$.

Definition 3.2.1. (Regular stable component) A regular stable component is defined to be a connected set in the two-parameter plane in which there is regular stable dynamics (and no stable chaotic dynamics). This is a set measured by Lyapunov exponents.

Definition 3.2.2. (Regular stable periodic component) A regular stable periodic component is defined to be a regular stable component such that the regular dynamics is periodic. The isoperiodic diagrams of Gallas measure this type of set.

Definition 3.2.3. (Shrimp) We define a shrimp to be a regular stable periodic component such that for each fixed value of parameter a (or b), the closure of each component contains infinitely many period-doubling bifurcations. Note that for that fixed parameter, each component can typically only contain one period-doubling cascade, since the parameter after the limit of cascade will be chaotic. Note that as in definition, each cascade component is a period-k cascade component, where k is the lowest period such that the component contains orbits of period $k \times 2^n$ for every $n = 0, 1, 2, ...$

Definition 3.2.4. (Shrimp nucleus) A shrimp nucleus is defined to be the subset of the shrimp consisting of the branch of period-k points, where the cascade is a period-k cascade.

Note that frequently but not always this shrimp nucleus is bounded on one side by a period- doubling bifurcation and on the other side by a saddle-node bifurcation. This is not the only possibility. For example, a period-k branch can be in two cascade components. For example, for parameter increasing, there could be a cascade, and for parameter decreasing there is also a cascade. See Figure 3.2. In addition, there could be saddle node on both ends, even though eventually a cascade will form on one end. For details about this case, refer to [4]. See also [41] for a scenario where these regions can be bounded by a saddle-node bifurcation and a torus bifurcation. A coupled system of

logistic map is studied in [24] and they have observed that the appearance of a shrimp implies the period-bubbling cascades (we call them bounded paired cascades) but the reverse is not true. We will explore it for the maps discussed in this chapter in the future.

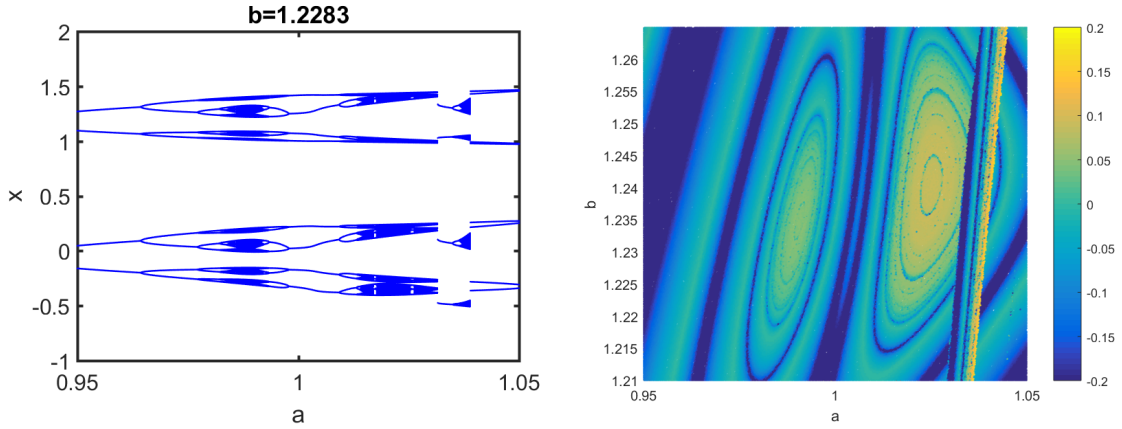

Figure 3.2: In the left picture, bounded paired cascades for $f(x)$ for a value of parameter b are shown. This means that there two cascades in the same connected component. In the right figure, the Lyapunov graph is shown for $f(x)$ for the values of parameters a, b for which the bounded paired cascades exist. Positive values (yellow) corresponds to chaos, and the negative values (more blue) corresponds to stable behavior. The left figure shows the stable dynamics along a fixed horizontal line in the right figure. The low period orbits on the left correspond to blue regions on the right. Note that although this is a shrimp, it is not typical since it does not have any legs emanating form the shrimp body.

Definition 3.2.5. (Shrimp spine) The shrimp spine is a set of superstable points when its is contained inside the shrimp nucleus.

In [6] the shrimp spine in one dimensional maps has been previously described as follows : The spine locus corresponds to parameter values that give rise to superstable orbits. Note that the shrimp spine is only guaranteed to exist if there is in fact a saddle-node bifurcation on one end and a period doubling bifurcation on the other. Also, this is only sufficient in one dimension, since in higher dimensions, there are non-real eigenvalues possible that would avoid this case. That is, in higher dimensions, an eigenvalue can change from -1 to 1 without ever crossing 0.

Most of the previous work has relied on numerical observations, See 3.3. Based on the results from Chapter 2 we are able to give theoretical results about the configuration of shrimps. To the best of

our knowledge, these are first results which guarantee the existence of shrimps based only on the existence of a parameter value at which there is no chaos and another parameter value with a regular stable periodic component.

Theorem 3.2.6. *Let $f(\lambda, x) : \mathbb{R} \times \mathcal{M} \to \mathcal{M}$ be a smooth two parameter map, where $\mathcal{M}$ is a smooth n-dimensional space and $\lambda \in \mathbb{R}^2$. Assume that for all parameters the periodic points lie in a compact set of $\mathcal{M}$. Let (a_0, b_0) be parameter pair at which f has either no periodic orbits or finitely many periodic orbits. Let (a_1, b_1) be a parameter pair at which there is chaos (that is it has positive periodic orbit entropy-defined as Definition 2.0.1). Then, any smooth curve between these two points is a one parameter family of maps and an arbitrary small perturbation of this curve has infinitely many windows. Additionally, if at (a_1, b_1), f is a k-map (as defined in Chapter 2), then using the enumeration scheme given in Chapter 2, we can also give a lower bound for each k, on how many period-k windows are there.*

Proof. It has been proved in Theorem 2.1.10 that a generic one parameter family of maps which has the property that for a sufficiently small value of the parameter, there are no or finitely many periodic orbits and for a sufficiently large value of a parameter, there are infinitely many regular periodic orbits, has infinitely many cascades. Since each of these cascades is connected to a periodic window. Therefore, there are infinitely many periodic windows. Since in one dimension, the periodic windows contain regular stable periodic orbits. Hence according to our definition of a shrimp, each of these windows in one parameter families of maps correspond to a shrimp in the two parameter space. Therefore, an arbitrary perturbation of a smooth curve in the parameter space will intersect infinitely many shrimps. □

3.3 Numerical shrimp detection

In this section, we give a summary of the methods used in the past for detecting shrimps. Specifically the methods that have been used are: the isoperiodic method, the continuation method, the superstable detection method and the Lyapunov exponent method. We describe each of these methods, and in particular we give full details for the Lyapunov exponent method, which is the method

we are using in our computations. Note that each of these methods detect a different form of object: namely, Lyapunov exponents detect regular stable components. The isoperiodic methods detect the regular stable periodic components. None of these methods detect the shrimp. Thus in order to guarantee that the object found is a shrimp additional work must be done. The continuation method detects the shrimp nucleus and the superstable detection method detects the shrimp spine.

In [19] Hoff et al, have studied a four dimensional four parameter Chua model and have used continuation methods as used in [12] to find the boundaries of exoskeletons of shrimps which we call shrimp nucleus. In [51] the authors have studied the Keller-Miksis equation and have also used the method of continuation to describe the shrimp shaped domains. In [8], the parameter space of a parametric perturbation of Rulkov map is investigated using the method of Lyapunov exponents and shrimp-shaped structures are characterized. Hassell map is studied by the authors in [9]. They have used the method of Lyapunov exponent and have discussed the exteming curves. Organizing curve of the shrimps is a concept that is discussed in many of the cited papers, in which a single smooth curve/line passes through the center of a whole set of the shrimp. In [9] it is observed that the curve is found using the superstable orbits.

Lyapunov exponents have been used by many authors. See [43, 54]. In [39], the dynamical properties of a dissipative kicked rotator are studied. The parameter space is studied using Lyapunov exponents and a comparison between bifurcation diagrams and the Lyapunov graphs is made. They have observed that infinite families of shrimp structures appear corresponding to periodic attractors and also calculated the Feigenbaum constant numerically in the case of strong dissipation. All the results are based on numerical observations and no theoretical statements were made. Shrimps have been observed to be organized in a particular way described along a straight line, however this line is dependent on the system used. See [15] for a similar calculation for the Henon map. We have not studied how the shrimps organize in the parameter spaces of maps we have considered but would be interested in learning about it in the future.

Gallas used isoperiodic diagrams to investigate the parameter space of the family of cubic maps [16] and the parameter space of the Henon map [15]. Note that this method is in fact a detection method for regular stable periodic components that we defined in Definition 3.2.2 above. In order to

guarantee that there are period-doubling cascades, extra work must be done. The parameter regions were investigated numerically for stable periodic orbits and was seen to contain many shrimp-like structures aligned along very specific simple directions. Shrimps are seen to correspond to islands of periodicity and to find the boundaries of such islands, the multiplier was used. For a period-k orbit the multiplier m is defined by $m = f'(x_{k-1})f'(x_{k-2})...f'(x_0) = (f^k)'(x_0)$ by chain rule. If $M \equiv |m|$, then the period-k orbit is attracting if $M < 1$, repelling if $M > 1$ and indifferent if $M = 1$. Superstable orbits are those for which $M = 0$, since this implies $f'(x_k) = 0$ for some point in the orbit. In parameter space the boundaries of k-periodic cells of stability are obtained by sweeping the parameters and recovering the values for which $m = 1$ (saddle-node bifurcation and for which $m = -1$ (flip or period doubling bifurcations).

Definition 3.3.1. (Lyapunov exponent) Let f be a smooth map of the real line. The Lyapunov number $L(x_1)$ of the orbit $\{x_1, x_2, x_3, ...\}$ is defined as

$$L(x_1) = \lim_{n\to\infty} (|f'(x_1)|...|f'(x_n)|)^{1/n},$$

if this limit exists. The Lyapunov exponent

$$\lambda = \lim_{n\to\infty} (1/n)(\ln|f'(x_1)| + ... + \ln|f'(x_n)|)$$

if this limit exists.

Observe that Lyapunov exponents are related to $\ln|m|$. The Lyapunov method generalizes to higher dimension. See [2]. In [49] the authors discuss the shrimp generation and their organization in the parameter space. It is shown that even though the geometric form of shrimps and their building principle are universal features but their spatial organization depends on individual system characteristics. It is illustrated in the case of Henon map. In [12] bifurcation structures in the case of two dimensional maps is discussed. For one dimensional maps with two parameters superstable orbits are stable and therefore are suitable to find the boundaries of shrimps. This method however does not work for the higher dimensional maps. In [12] continuation methods combined with the

results on stability of cycles in higher dimensional maps are introduced to determine the bifurcation structures.

We will use the method of Lyapunov exponents to study the dynamics of two parameter maps.

The Lyapunov exponent measures the rate of separation of trajectories starting from points very close to each other in phase space. Therefore it measures sensitivity to initial conditions. If $\lambda < 0$ the orbit is stable. The orbit is superstable ($m = 0$) if $\lambda = -\infty$. If $\lambda > 0$, the orbit is unstable and exhibits sensitivity to initial conditions. The Lyapunov graphs are constructed by numerically computing the Lyapunov exponent and is then plotted using colors as a function of the parameters of the maps. We use a fixed initial condition for the calculation of Lyapunov exponents in all the figures except for Figure 3.7. The parameter values are chosen randomly from a grid of values. In [14] the dynamics of the circle map are studied using the Lyapunov graph in the space of parameters. Lyapunov graph method has been used in the case of one dimensional one parameter maps (see [45] and [25]) as well as two parameter maps (see [14]). Shrimps have also been found using the Lypaunov graph method in higher dimensional maps as well (see [12], see also Figure 3.3, where we have computed the Lyapunov exponents for the Henon map).

We have used the Lyapunov graph method to draw the parameter space diagrams in the case of the cubic map (see Figure 3.1) and Henon map (see Figure 3.3) first observed by Gallas and Milnor.

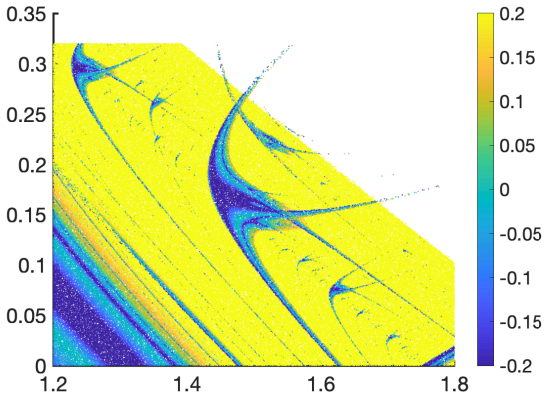

Figure 3.3: Lyapunov graph for the Henon map $H_{a,b}(x, y) \to (a - x^2 + by, x)$ is shown for parameter values $1.2 \leq a \leq 1.8$ and $0 \leq b \leq 0.32$. The blue regions with multiple legs are all shrimp regions. This is a measure of the largest Lyapunov exponent.

In the next sections, we give two more examples of two parameter maps, not discussed before and use Lyapunov graphs to numerically show that shrimps exist. We also relate the one parameter bifurcation diagrams to the configuration of the shrimps. We apply the results from Chapter 2 to the previously discussed family of cubic maps and use Theorem 3.2.6 to conclude that our numerical results are uncovering actual shrimps (at least for an arbitrarily small perturbation of the map) for the degree 3, 5, and 6 polynomial maps.

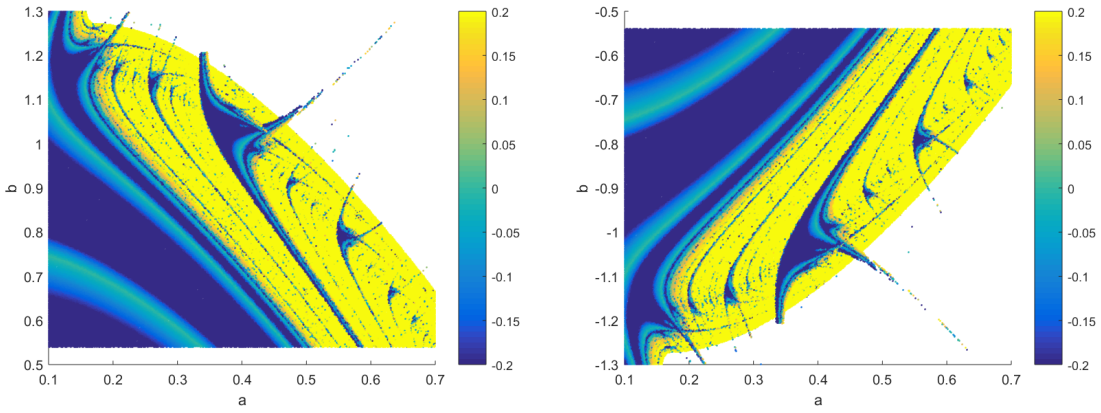

Figure 3.4: Lyapunov graph for the cubic map $f(x) = -x^3 + 3ax - b$, two magnifications of Figure 3.1

3.4 Shrimps in the cubic map

In this section we study the previously discussed family of cubic maps, $f(x) = -x^3 + 3ax - b$. Shrimps were found in this family of cubic maps by many authors, for example, Milnor [31] was the first one to observe swallow shaped regions in the parameter space of the cubic family of maps. Gallas also studied the isoperiodic diagrams of the cubic map and found shrimp like structures in the parameter space of the cubic map, see [16, 17]. In this section we give more detailed bifurcation diagrams for a single parameter and also describe the relation between the appearance of periodic windows (See Definition 2.1.4) in the bifurcation diagrams and the configuration of shrimps in the parameter space. We use the method of Laypunov exponents to draw the parameter space diagrams.

In Figure 3.5, we compare the bifurcation diagram of the cubic map $f(x) = -x^3 + 3ax - b$ drawn for $b = 0.66465$ and varying a with the Lyapunov graph of $f(x)$. The Lyapunov graph shows the shrimps along with their periods. In Figure 3.6, bifurcation diagrams for various values of the parameter b are shown with the periodic windows. The horizontal lines in the Lyapunov graph correspond to the b values used in the bifurcation diagrams.

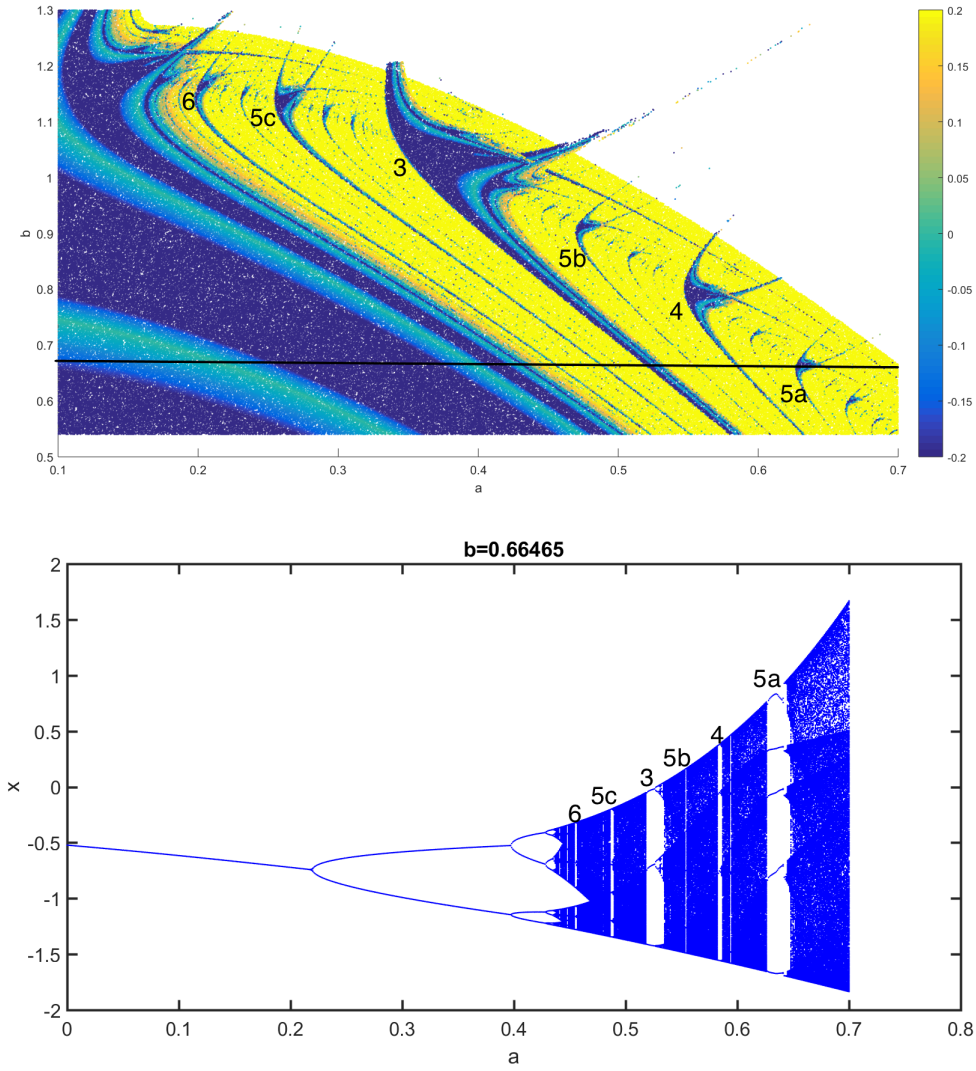

Figure 3.5: In the top figure, the periods of the shrimps appearing in the parameter space of $f(x) = -x^3 + 3ax - b$ are marked. The horizontal line represents the parameter value $b = 0.66465$. In the bottom figure, the bifurcation diagram for the cubic map $f(x) = -x^3 + 3ax - b$ is shown. a is being varied and $b = 0.66465$. The numbers in the figure represent the period of the periodic windows. We have used a fixed initial condition $x_0 = 0$. The graininess of the picture is because the parameters are chosen randomly from a grid of values in the algorithm.

The order of the appearance of shrimps corresponds to the order in which periodic windows appear in the bifurcation diagram. For example, the periodic window marked $5a$ in the left figure corresponds to the shrimp marked $5a$ in the right figure. As the parameters are varied the location

of these windows change. There are other shrimps and periodic windows between the ones marked in these pictures but they can be very small and hence sometimes cannot be seen in these figures.

There is strong relationship between shrimps in two parameters families and windows in one parameter families. Specifically if there is a shrimp in the two parameter diagram, as defined by our definition, then for any fixed parameter b which intersects a k-shrimp for a range in (a_1, a_2), there is a stable period-k window for (a_1, a_2). In fact, even if we create a curve in the two parameter space which does not hold b fixed, then f restricted to this curve is a one parameter family. There is certainly a regular stable periodic window that occurs exactly at the range where the curve intersects the shrimp. We need to use further reasoning to show that the one parameter family contains a period doubling cascades. Theorem 2.1.10 gives a result in this direction.

For example, for the cubic map, for $a = 0$, there is only a single fixed point with negative derivative and there are no other fixed or periodic points. One can find a pair of values of (a_1, b_1) for which the cubic map is a 3-map. This has been proved by Sander and Yorke in Corollary 4 in [47]. Therefore given any curve between $(a, b) = (0, b)$ and (a_1, b_1) the theorem says that arbitrary small perturbation of this curve intersects an infinite number of shrimps and using the results of [21], for every k we can find the number of k-shrimps bounded below by the number given in the Table 3.1. The table below shows the values for $k = 1$ to $k = 7$.

Table 3.1: The number of regular period-k orbits for the $cubic$ family of maps.

(m, j)	$k = 1$	$k = 2$	$k = 3$	$k = 4$	$k = 5$	$k = 6$	$k = 7$
(3,1)	1	1	4	8	24	56	156

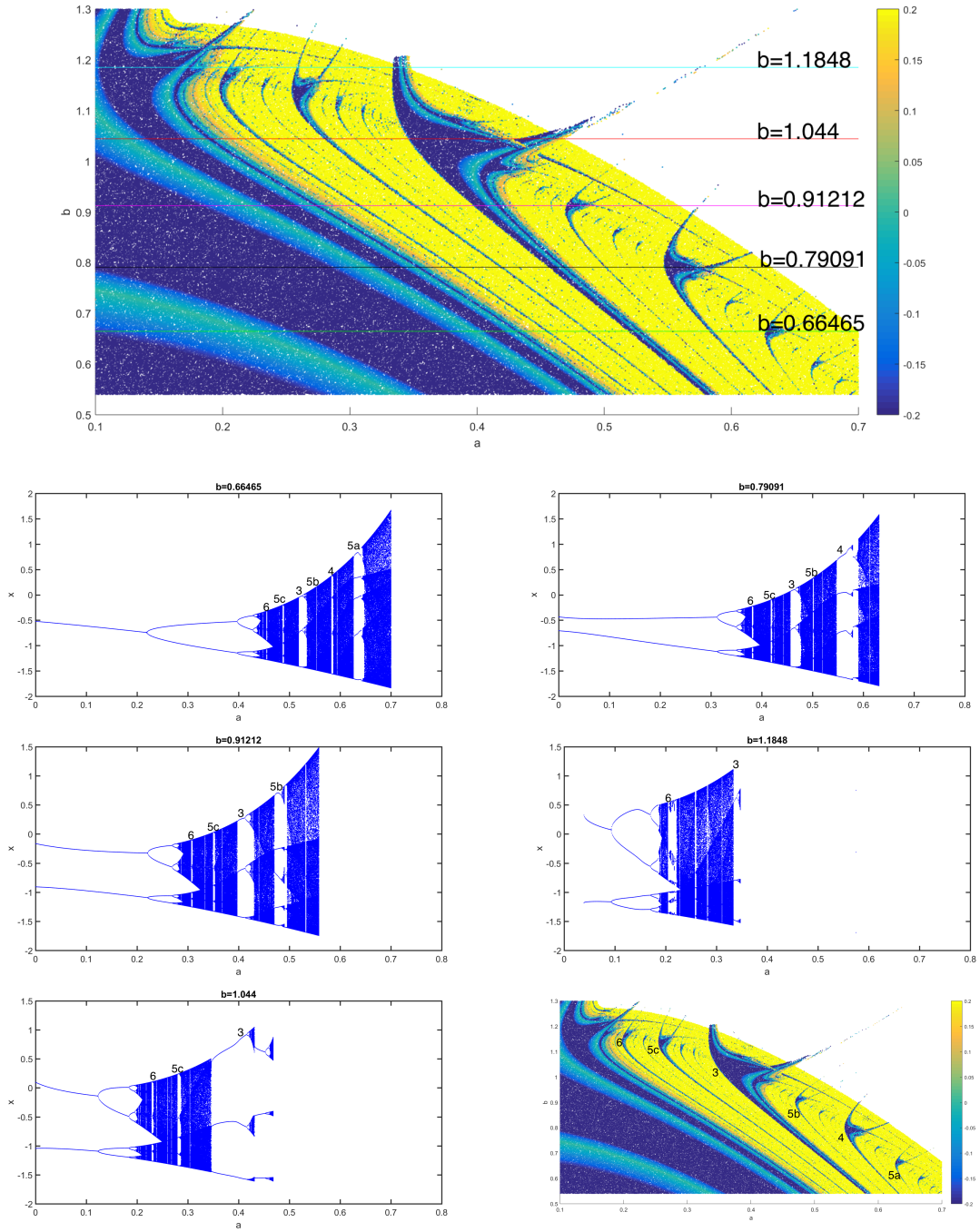

Figure 3.6: Bifurcation diagrams of the cubic map $f(x) = -x^3 + 3ax - b$, for some fixed values of b and the two parameter Lypaunov graph for $f(x)$. Each horizontal line in the Lyapunov graph represents the value of parameter b used in the bifurcation diagrams. The locations of shrimps in the Lyapunov graph correspond to the locations of periodic windows in the bifurcation diagrams. The initial condition used is $x_0 = 0$. The graininess of the picture is because the parameters are chosen randomly from a grid of values in the algorithm.

3.5 Shrimps in the quintic map

In Chapter 2, specifically in Theorem 2.5.1, we proved that a large scale perturbation of one parameter degree five polynomial map is a 5 map. In this section we discuss the following two parameter family of degree five maps

$$f(x, a, b) = x^5 - 3ax^3 + a^2x + b$$

and show that the periodic windows in the one parameter family of the degree five polynomial maps and the shrimps in two parameter degree five polynomial map are strongly connected. In the Figure 3.7, the Lyapunov graph for $f(x)$ shows the collection of shrimps in the parameter space calculated using three different values of the initial condition. The structure in the parameter space is affected by the change in the initial condition, however the locations of the shrimps in the chaotic regions remain unaffected. The shrimps are symmetrically arranged on the two sides of the $b = 0$ line since $f(-x, a, -b) = -f(x, a, b)$. Figure 3.8 shows the magnified view of the upper half of Figure 3.7. One may think that the complexity of the structures observed in the parameter space depends on the non linearity of the parameters in the map, however this is not the case. The structure seen in the Lyapunov graph of the cubic map $f(x) = -x^3 + 3ax - b$, has similar complexity even though all the parameters appear with a linear power.

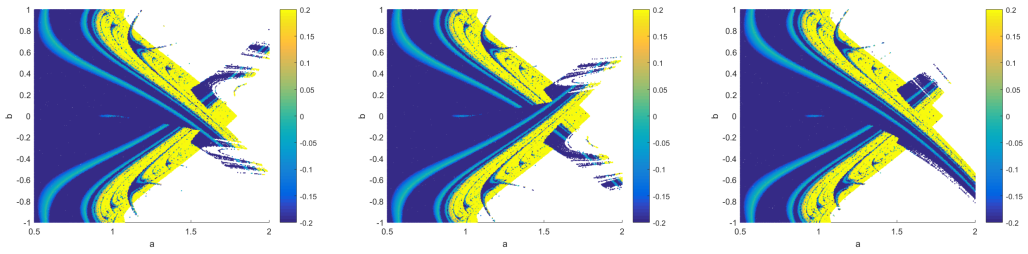

Figure 3.7: In this figure, the Lyapunov graph is shown for the $f(x) = x^5 - 3ax^3 + a^2x + b$ for three different values of the initial condition. In the left figure, $x_0 = 0.1$. In the central figure, $x_0 = -0.1$. In the right figure, a random initial condition is used.

$f(x)$ is the *quint* map with $g(\lambda, x)$ replaced with b. Therefore the conditions of Theorem 2.5.1 still hold, and there exist a pair of values (a_0, b_0) such that there is a unique fixed point and no other

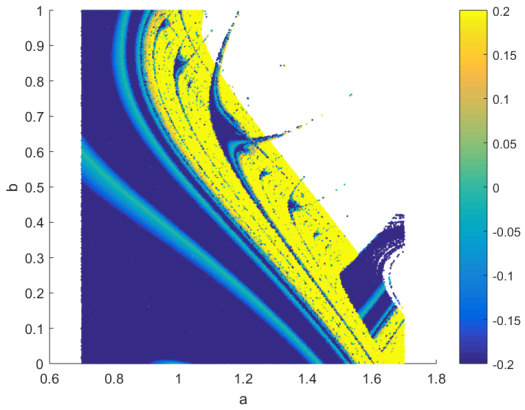

Figure 3.8: In this figure, the magnified view of the upper part of Lyapunov graph is shown for the $f(x) = x^5 - 3ax^3 + a^2x + b$.

periodic points exist. And another pair of values (a_1, b_1) such that $f(x)$ is a 5-map. Hence, from Theorem 3.2.6, an arbitrary small perturbation of any curve between (a_0, b_0) and (a_1, b_1) intersects an infinite number of shrimps.

In Figure 3.9, we show that the above is true by comparing the bifurcation diagrams with the Lyapunov graph. The period of each window in the bifurcation diagrams is marked and the corresponding b values with the period of shrimp are marked in the two parameter diagram. It is clear from the figures that if there is a shrimp in the two parameter diagram, then for any fixed parameter b which intersects a k-shrimp for a in range (a_1, a_2), there is a stable period-k window for (a_1, a_2). In fact since this map is a 5 map, we can find a lower bound for the number of k-shrimps using the Table 2.2. Not all shrimps and windows are visible because most of the shrimps and windows are very small in size. An interesting feature that is observed in the phase space bifurcation diagram of $f(x)$ is the appearance of bounded paired cascades for some values of the parameters (see definition in Chapter 2). It is also observed that in the case of two parameter degree five polynomial maps, the shrimps do not have the typical shape for the values of parameters where there are bounded paired cascades. See Figure 3.2. We will explore the reason for this change in the shape of a shrimp in our future work.

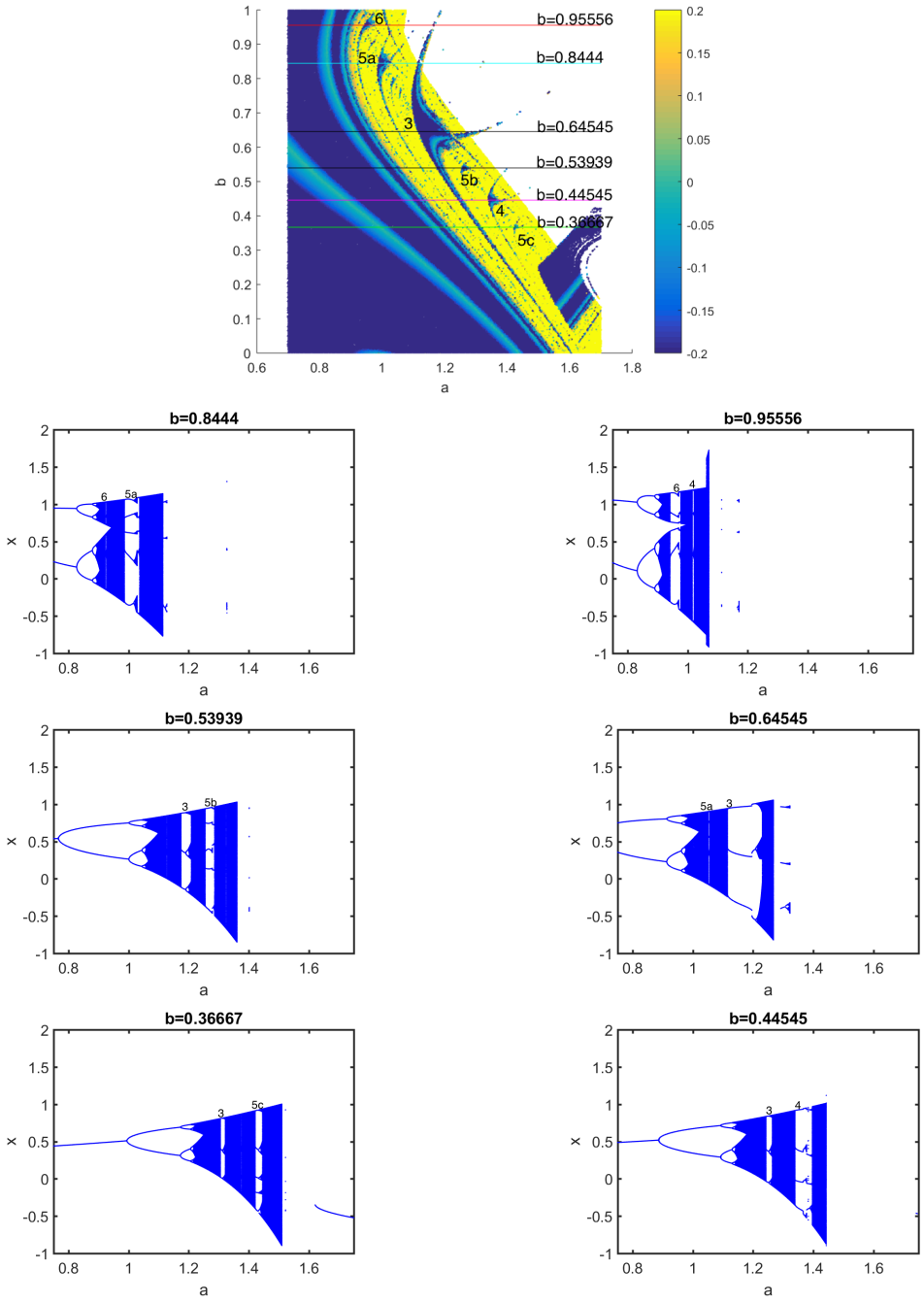

Figure 3.9: In these figures the bifurcation diagram for the two parameter map $f(x) = x^5 - 3ax^3 + a^2x + b$ is shown for different values of the parameter b while a is being varied. Notice that the location of periodic windows in the bifurcation diagrams corresponds to the location of shrimps in the two parameter diagram. The values for b from these bifurcation diagrams are marked by a horizontal line in the Lyapunov graph and the periods of each shrimp are also shown.

3.6 Shrimps in the degree six map

In Chapter 2, specifically in Theroem 2.5.2, we proved that a large scale perturbation of one parameter degree six polynomial map is a 6-map. In this section we discuss the following two parameter family of degree six maps

$$f(x) = x^6 - 3ax^4 + 2a^2x^2 + b - \frac{a^3}{5},$$

and show that the periodic windows in the one parameter family of degree six polynomial maps and the shrimps in two parameter degree six polynomial map are strongly connected. The lyapunov graph in Figure 3.10 shows the shrimps in the parameter space.

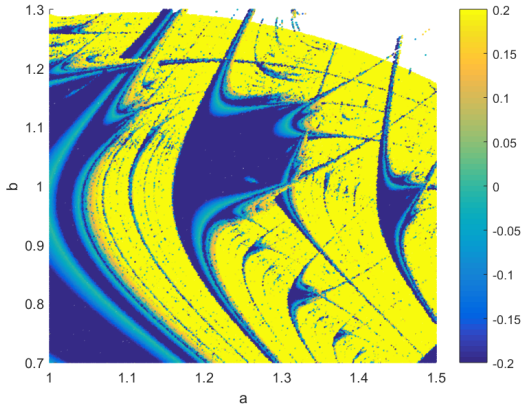

Figure 3.10: In this figure, the Lyapunov graph is shown for the $f(x) = x^6 - 3ax^4 + 2a^2x^2 + b - \frac{a^3}{5}$. The color is the Lyapunov exponent. Therefore, the positive values (more yellow) corresponds to chaos, and the negative values (more blue) corresponds to regular behavior. The white space is the parameter values for which there is no stable behavior. The initial condition is $x_0 = 0.1$. Note the large number of legs on the shrimp.

If we compare the phase space bifurcation diagrams for certain values of parameter b with Lyapunov graph for $f(x)$, we see that the conclusion from the previous two sections still holds true. In Figure 3.11, the periodic windows for $b = 0.74848$ are shown and the corresponding shrimps of the same period are marked in the two parameter diagram. In Figure 3.12, the bifurcation diagrams

are shown for multiple values of b. The horizontal lines depicting b values from the bifurcation diagrams correspond to the approximate locations of shrimps in the parameter space for $f(x)$. Since $f(x)$ is equal to the hex map with $g(\lambda, x)$ replaced with b, the conditions of Theorem 2.5.2 still hold true. Therefore, we can find a pair of values (a_0, b_0) such that there are no fixed points or periodic orbits and a pair of values (a_1, b_1) such that this is a 6-map. Hence by Theorem 3.2.6, an arbitrary small perturbation of the curve joining these points will intersect infinitely many shrimps. In fact since this map is a 6 map, we can find a lower bound for the number of k-shrimps using the Table 2.3.

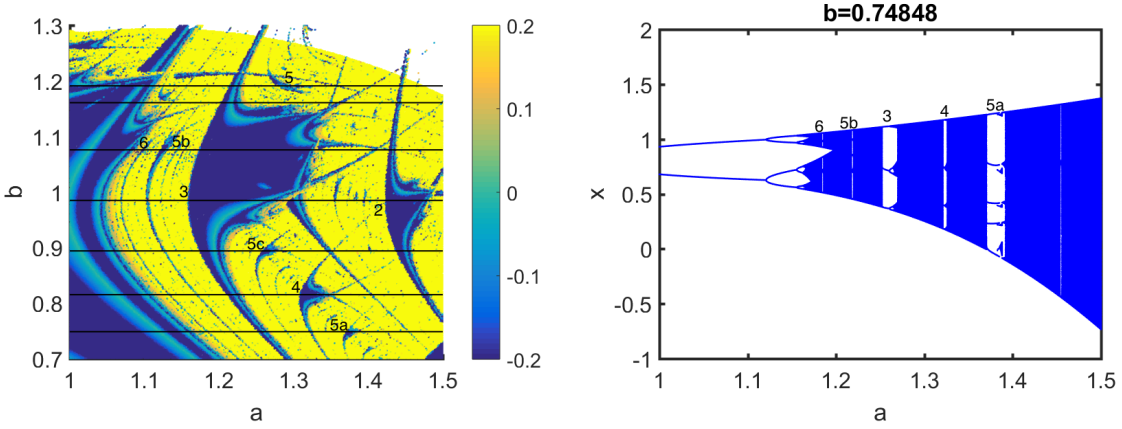

Figure 3.11: In the left figure the Lyapunov graph for $f(x) = x^6 - 3ax^4 + 2a^2x^2 + b - \frac{a^3}{5}$ is shows with the periods of shrimps in the parameter space. In the right figure, the bifurcation diagram for the same map is shown. a is being varied and $b = 0.74848$. The numbers in this figure represent the period of the periodic windows. The horizontal line $b = 0.74848$ in the Lyapunov graph intersects the shrimps of periods $5a, 4, 3, 5b, 6$. The intersections correspond to the a values in the bifurcation diagram where the periodic window of the same period appears.

Another property revealed by the Lyapunov graphs is the existence of bistability at the parameter values where the legs of shrimps intersect. For example, in the Lyapunov graph of the degree six polynomial map, at $(a, b) = (1.338, 0.81515)$, two distinct stable period-4 orbits exist. This point also refers to the intersection of two legs of the period 4 shrimp. Similarly, at $(a, b) = (1.355, 1.1909)$ one stable period 3 orbit and one stable period 2 orbit exist. A discussion of the coexistence of attractors for the logistic map is given in [26].

Another important observation we make from the Lypaunov graph of $f(x)$ is that the complexity of the shrimps has gone up. Looking at the shrimp in the center of Figure 3.10, one can see that the number of legs is more than the number of legs in the shrimps observed in other maps. We do not yet know the reason for that, and is something we want to pursue in the future. We conjecture that as the number of critical points (points where the map has zero derivative) increases, the numbers of legs observed in the shrimps also increases. It may also be related to the non linearity of the variable in the map but more work needs to be done to establish this fact.

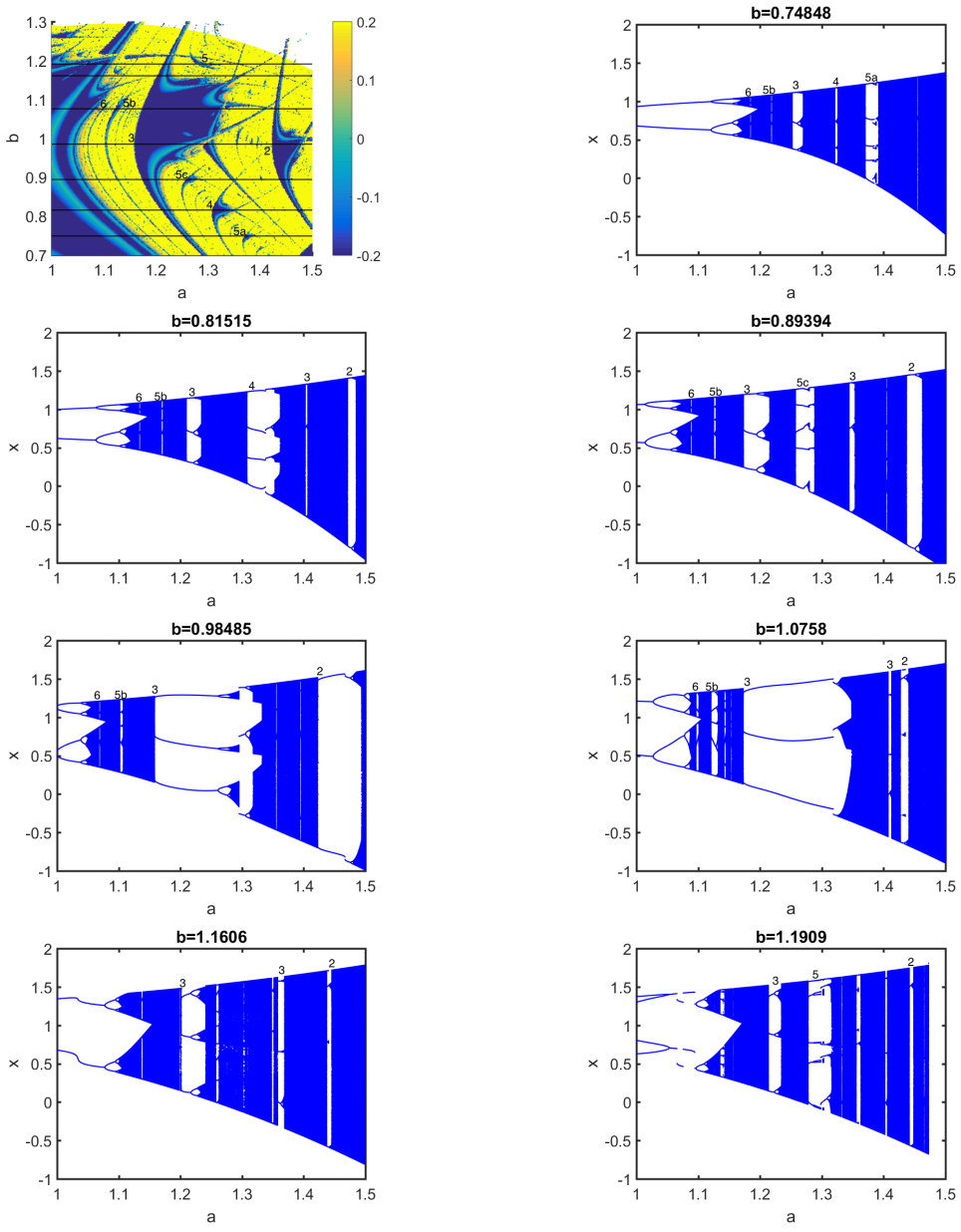

Figure 3.12: In these figures the bifurcation diagram for the degree six map $f(x) = x^6 - 3ax^4 + 2a^2x^2 + b - \frac{a^3}{5}$ is shown for different values of the parameter b while a is being varied. Each of bifurcation diagrams show the periodic windows with their periods. The values for b from these bifurcation diagrams are marked by a horizontal line in the Lyapunov graph.

3.7 Population model

Period doubling cascades have been observed in many population models. In [42] Previte and Hoffman look at the Predator-Prey model by introducing a third scavenger species to the classical predator-prey equations in a biologically reasonable way. The third species is characterised as a scavenger who is also a predator of the prey and scavenges the carcasses of the predator. They show that in addition to having the relevant property of bounded trajectories for positive initial conditions this model exhibits Hopf bifurcations, bistability and chaos indicating the complexity of the dynamics due to adding a scavenger to a classical predator prey system.

In [50] the dynamics of an overcompensatory Leslie population model was studied by Ugarcovici and Weiss, where the fertility rates decay exponentially with population size. They studied the two and three dimensional models and found a variety of complicated behaviour, including period doubling cascades.

In [27] two discrete single population models with overcompensating density-dependence and Allee effects due to predator saturation and mating limitations are analysed using symbolic dynamics. They focus on the scenarios of persistence and bistability, in which the species dynamics can be chaotic. They compute topological entropy and Lyapunov exponent under ecological key parameters and different initial conditions. The models investigate in their study can be represented with the following general difference equation:

$$N_{n+1} = N_n e^{r(1-N_n/K)} \beta(N_n)$$

where $e^{r(1-N_n/K)}$ is a negative density-dependent factor and the term $\beta(N_n)$ is used to introduce a positive density-dependent factor. Here r is the intrinsic growth rate and K is the carrying capacity. We will focus on the model with Allee effects due to predator saturation. In this case, $\beta(N) = e^{-m/(1+sN)}$. Here $\beta(N)$ corresponds to the probability of escaping predation by a predator with a saturating functional response, being m the intensity of predation and s a parameter proportional to the handling time. By non-dimensionalizing the above equation by taking $x_n = N_n K^{-1}$, we obtain

the model under study, given by

$$x_{n+1} = x_n exp\left(r(1 - x_n) - \frac{m}{1 + sKx_n}\right)$$

This system undergoes period-doubling route to chaos. Under the selected parameter values, if the handling time (sK) is increased, chaos emerges, but at a critical value the population collapses and enters the essential extinction scenario. An increase in the intensity of predation, m, stabilizes the dynamics, although for large values of m the population becomes extinct due to entry into the scenario of extinction. If r is varied, then we see a similar behavior as with varying handling time, that is, after the saddle-node bifurcation the population reaches a nontrivial steady state and after a flip bifurcation, the population achieves chaos via period-doubling cascade, and then collapses into essential extinction. The bifurcation diagrams for these three cases are shown below.

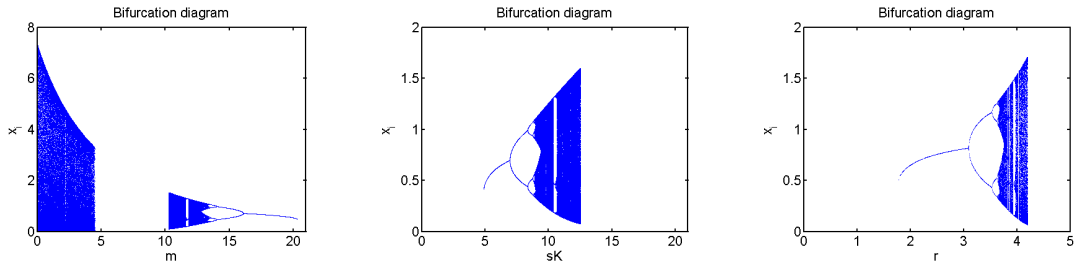

Figure 3.13: In this figure, the bifurcation diagrams for the population model are drawn by varying one parameter and keeping the other two constant. For the left picture, m is varied and $r = 4.5$, $sK = 16$. In the middle picture, sK is varied and $r = 4.5$, $m = 8$. In the right picture, r is varied and $m = 8$, $sK = 16$.

They calculate the topological entropy using kneading theory and by using the theory of unimodal maps. Topological entropy measures the complexity of the system. Let f be an iterated map on the interval $I = [a, b]$, which is a 2-piecewise monotone map with one turning point c. Therefore,

the interval I is divided into the following sets:

$$I_L = [1, c], \qquad I_{c^*} = \{c\}, \qquad I_R = [c, b]$$

so that f restricted to the interval I_L is strictly increasing and f restricted to interval I_R is strictly decreasing. Each of these subintervals is called a lap of f, and the number of distinct laps $l = l(f)$, is called the lap number of f. Let $O(c) = \{x_i : x_i = f^i(c), i \in \mathbb{N}\}$. Associate to each orbit $O(c)$ a sequence of symbols, which leads to the itinerary $(i(x))_j = S = S_1 S_2 \dots S_j \dots$, where $S_j \in \mathbb{A} = \{L, C^*, R\}$ and

$$\begin{aligned} S_j = L \quad & if \quad f^j(x) < c, \\ S_j = C^* \quad & if \quad f^j(x) = c, \\ S_j = R \quad & if \quad f^j(x) > c. \end{aligned}$$

The concept of kneading increments and kneading-matrix was introduced by Milnor and Thurston [32]. The kneading matrix of an interval map is defined to be a matrix whose entries are elements of $\mathbb{Z}[t]$, the ring of formal power series with integer coefficients. The kneading increments are power series that measure the discontinuity evaluated at the turning points c_i, $i = 1, 2, \dots, m$, of m-modal maps. For the case of unimodal maps, we have one kneading increment defined by $v(t) = \theta_{c^+}(t) - \theta_{c^-}(t)$, where $\theta_x(t)$ is the invariant coordinate of the sequence $S_0 S_1 S_2 \dots S_j \dots$ associated to the itinerary of the point x. $\theta_x(t) = \sum_{j=0}^{\infty} \tau_j t^j S_j$, where $\tau_j = \prod_{i=0}^{j-1} \epsilon(S_i)$ for $j > 0$, $\tau_0 = 1$ for $j = 0$, $\epsilon(S_i) = \begin{cases} -1 & \text{if } S_i = R \\ 0 & \text{if } S_i = C^* \text{ and } \theta_{c^\pm}(t) = \lim_{x \to c^\pm} \theta_x(t). \\ 1 & \text{if } S_i = L \end{cases}$

Taking the kneading sequence $RLLLLLLRRLLC$ obtained from $m = 4$ and $sK = 9.365$ (with

$r = 4.5)$ with period 12, they illustrate the computation of topological entropy. The kneading-matrix $N(t)$ is computed and the corresponding kneading determinant, $D(t)$. The topological entropy of f, is given by $h_{top}(f) = \log s$, where s is the growth number of a unimodal interval map, and is given by $s = 1/t^*$, t^* being the root of $D(t)$, which has the lowest modulus. In this case $t^* = 0.502140...$, and the topological entropy is given by

$$h_{top}(f) = \log\left(\frac{1}{t^*}\right) = 0.688874..$$

They also computed the topological entropy using sK and m as control parameters, and found out that the topological entropy is positive once the dynamics falls into chaotic semistability, which are the values of the parameter for which a period doubling cascade exists. For m =4, 8, and 12, the topological entropy is computed for growing sK and it is observed that the topological entropy increases with increase in sK and it is maximum for $sK \approx 13$. The values of entropy at increasing predation intensity, m are similar. With sK=12, it is shown that for very small values of m, the topological entropy is positive because the dynamics is chaotic. Once the parameter reaches the critical value(for this case $m \approx 4$), the topological entropy is maximum and then it decreases. As m is increased further the topological entropy is diminished as the system undergoes the inverse period-doubling bifurcations.

The population model discussed above has multiple parameters m, sK and r. We decided to look for shrimps in the parameter space by varying two parameters and keeping one parameter constant.

$$f(x) = xe^{r(1-x)-\frac{m}{1+sKx}}$$

That is keeping r constant and varying both m and sK at the same time. No typical shrimps were found in the parameter space.

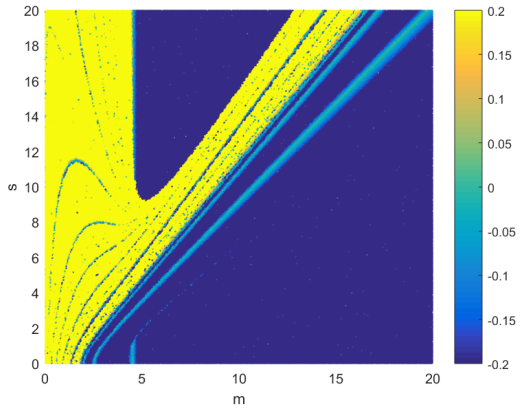

Figure 3.14: Lyapunov graph for population model is shown. Parameters sK and m are varied simultaneously and $r = 4.5$

It has been proved that topological entropy is monotonic for the family of quadratic maps (see [11,30,32]). Based on the results of [5], we conjecture that since the population model is unimodal, it is also monotonic. This means that periodic orbits do not disappear when the parameters are varied. And this is also the reason why we do not see typical shrimps with many legs in the parameter space. We also conjecture that typical unimodal maps do not have shrimps with multiple legs.

3.8 Conclusion and further research

In Chapter 3 we have shown the relation between one parameter bifurcation diagram and the shrimps observed in Lyapunov graphs for two parameter family of maps. We have also given a theoretical result for the abundance of shrimps in the parameter space of two parameter families of maps with infinitely many cascades. As far as we know, only results based on numerical observations have been given so far and none of them have discussed the connection between the bifurcation diagrams and Lyapunov graphs.

In our numerical explorations we made some interesting observations which we will be exploring further in the future. In the degree 3, 5 and 6 polynomial two parameter maps, we observed that each of these maps have bounded paired cascades for some parameter values in the phase space

bifurcation diagram. Exploring the Lyapunov graph for these values of the parameters gives different results in these cases. For example, in the degree five polynomial map, the shape observed for the parameter values for which bounded paired cascades exist is different from the typical shrimp shape. See Figure 3.2. On the other hand, in the case of the cubic and degree six maps, the typical shrimp shape is observed for these values. See Figure 3.15.

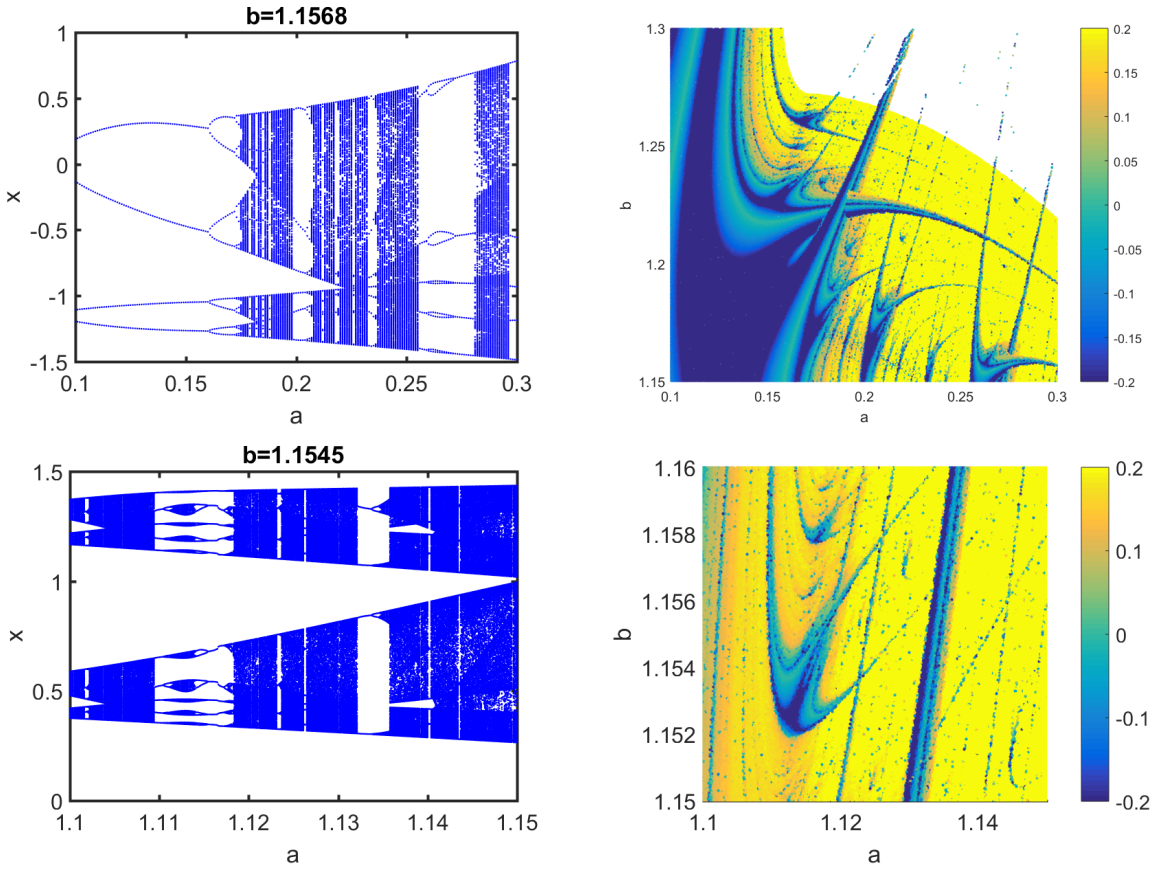

Figure 3.15: In the top two figures, the paired cascades and the shrimps for the corresponding values of the parameters are shown for the cubic map and the bottom two pictures show the same thing for the degree six polynomial map.

Another interesting observation we made is that the number of legs in the shrimps increase if the number of maxima or minima of the maps increase and it may also be related to the non linearity of the parameters in the map. To this end, we conjecture that the number of legs on a shrimp is

connected to the number of extreme values of a map. For example in Figure 3.10, the shrimp in the center has many legs. A typical shrimp has four legs. To test our conjecture, we drew Lyapunov graph for the following map $f(x) = a - x^2 + b\sin(2\pi x)$. This map has many extreme values and we observed that the complexity of shrimps has gone up. The shrimp in the center of the parameter space has more legs than a typical shrimp. It may also depend on the non linearity of the parameters used in the map but more work needs to be done to establish this fact.

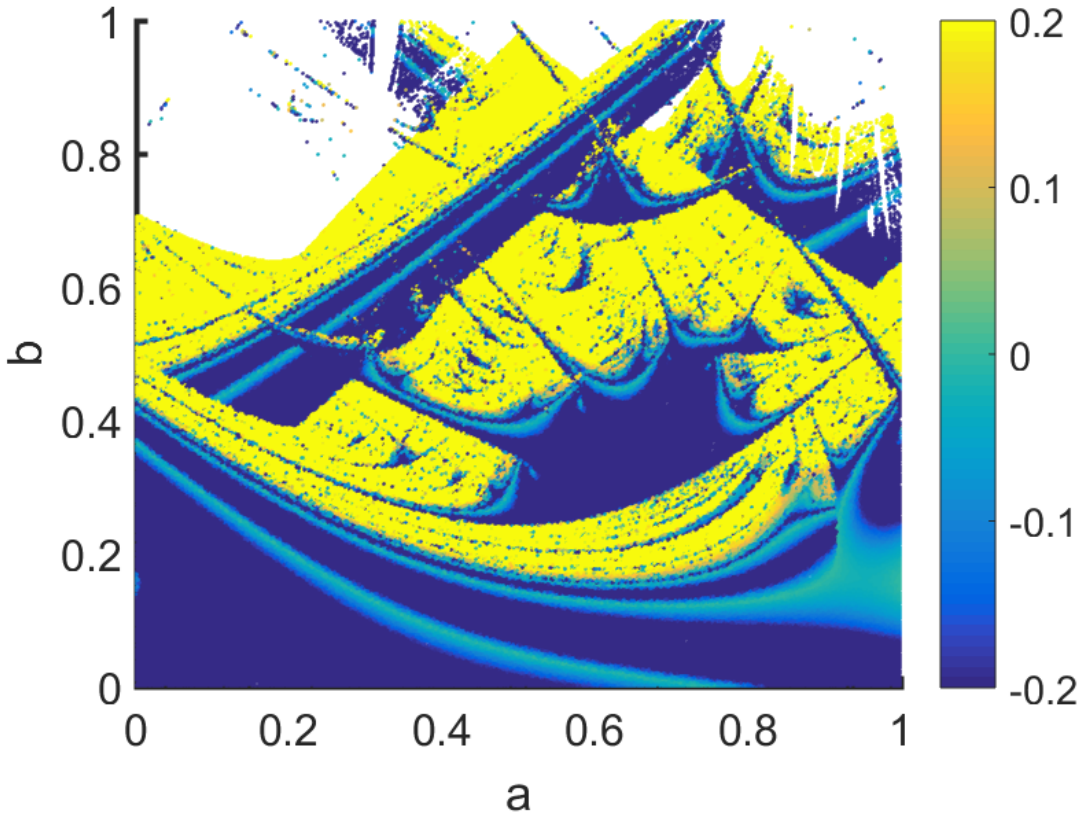

Figure 3.16: The Lyapunov graph for $f(x) = a - x^2 + b\sin(2\pi x)$ where a and b are parameters.

Bibliography

[1] Holokx A. Albuquerque, Rero M. Rubinger, and Paulo C. Rech. Self similiar structures in a 2d parameter space of an inductorless chua's circuit. *Physics letters A*, 372(27):4793–4798, 2008.

[2] Kathleen T. Alligood, Tim D. Sauer, and James A. Yorke. *Chaos An introduction to dynamical systems*. Springer, New York, 1997.

[3] José M. Amigó and Ángel Giménez. Entropy monotonicity and superstable cycles for the quadratic family revisited. *Entropy*, 22(10):1136, Oct 2020.

[4] Philip J Aston and Neil Bristow. Alternating period-doubling cascades. *Nonlinearity*, 26(9):2553–2576, aug 2013.

[5] Artur Avila and Carlos Gustavo Moreira. Statistical properties of unimodal maps: the quadratic family. *Annals of Mathematics*, 161(2):831–881, 2005.

[6] Ernest Barreto, Brian Hunt, C Greborgi, and James Yorke. From high dimensional chaos to stable periodic orbits: The structure of parameter space. *Physical Review Letters - PHYS REV LETT*, 78:4561–4564, 06 1997.

[7] H. Bruin and S. van Strein. Monotonicity of entropy for real multimodal maps. *American Mathematical Society*, 28, 2009.

[8] Diogo Ricardo da Costa, Matheus Hansen, and Antonio Marcos Batista. Parametric perturbation in a model that describes the neuronal membrane potential. *Physica A: Statistical Mechanics and its Applications*, 515:519 – 525, 2019.

[9] Juliano A. de Oliveira, Hans M.J. de Mendonça, Diogo R. da Costa, and Edson D. Leonel. Effects of a parametric perturbation in the hassell mapping. *Chaos, Solitons and Fractals*, 113:238 – 243, 2018.

[10] S.L.T. de Souza, A.M. Batista, M.S. Baptista, I.L. Caldas, and J.M. Balthazar. Characterization in bi-parameter space of a non-ideal oscillator. *Physica A: Statistical Mechanics and its Applications*, 466:224 – 231, 2017.

[11] A. Douady. Topological entropy of unimodal maps. *NATO ASI series*, 464, 1993.

[12] Wilson Façanha, Bart Oldeman, and Leon Glass. Bifurcation structures in two-dimensional maps: The endoskeletons of shrimps. *Physics Letters A*, 377(18):1264 – 1268, 2013.

[13] Mehmet Onur Fen and Fatma Tokmak Fen. Replication of period-doubling route to chaos in impulsive systems. *Electronic Journal of Qualitative Theory of Differential Equations*, (58):1–20, 2019.

[14] Julio Figueiredo and Coraci Malta. Lyapunov graph for two-parameters map: Application to the circle map. *International Journal of Bifurcation and Chaos*, 8:281–293, 02 1998.

[15] Jason Gallas. Structure of parameter space of the henon map. *Physical Review letters*, 70:2714–2717, 1993.

[16] Jason Gallas. Dissecting shrimps: Results for some one dimensional physical models. *Physica A*, 202:196–223, 1994.

[17] Jason A. C. Gallas, Fernando Cabral, and Alexandre Lago. A picture book of two families of cubic maps. *International Journal of Modern Physics*, 4(3):553–568, 1993.

[18] Anderson Hoff, Denilson T. da Silva, Cesar Manchein, and Holokx A. Albuquerque. Bifurcation structures and transient chaos in a four-dimensional chua model. *Physics letters A*, 378(3):171–177, 2014.

[19] Anderson Hoff, Denilson T. da Silva, Cesar Manchein, and Holokx A. Albuquerque. Bifurcation structures and transient chaos in a four-dimensional chua model. *Physics Letters A*, 378(3):171 – 177, 2014.

[20] Brian R. Hunt, Jason A. C. Gallas, Celso Grebogi, James A. Yorke, and H. Kocak. Bifurcation rigidity. *Physica D*, 129:35–56, 1999.

[21] M. R. Joglekar, E. Sander, and J. A. Yorke. Fixed point indices and period doubling cascades. *J. Fixed Point Theory Appl.*, 8:151–176, 2010.

[22] I. Kan, H. Kocak, and J. A. Yorke. Antimonotonicity: concurrent creation and annihilation of periodic orbits. *Annals of Mathematics*, 136:219–252, 1992.

[23] Matthew D. Kvalheim and Anthony M. Bloch. Families of periodic orbits: closed 1-forms and global continuability, 2019.

[24] G. C Layek and N. C Pati. Organized structures of two bidirectionally coupled logistic maps. *Chaos (Woodbury, N.Y.)*, 29(9):093104–, 2019.

[25] M. Markus. Chaos in maps with continuous and discontinuous maxima. *Computer in Physics*, 481(4), 1990.

[26] Mario Markus and Benno Hess. Lyapunov exponents of the logistic map with periodic forcing. *Computers and Graphics*, 13(4):553–558, June 1989.

[27] N. Martins and J. Sardanyés J. Duarte, C. Januário. On chaos, transient chaos and ghosts in single population models with allee effects. *Non linear Analysis: Real world applications*, 13(4):1647–1661, 2012.

[28] Robert May. Biological populations with nonoverlapping generations: stable points, stable cycles and chaos. *Science*, 186(4164):645–647, 1974.

[29] Robert May. The cubic map in theory and practice. *Mathematical Modelling*, 1984.

[30] W. De Melo and S. van Strein. *One dimensional dynamics*. Springer-Verlag, 1993.

[31] J. Milnor. Remarks on iterated cubic maps. *Experiment. Math.*, 1:5–24, 1992.

[32] J. Milnor and W. Thurston. On iterated maps of the interval. *Dynamical systems*, 1342:465–563, 1988.

[33] J. Milnor and C. Tresser. On entropy and monotonicity for real cubic maps. *Comm. Math. Phys.*, 209:123–178, 2000.

[34] M. Misiurewicz and W. Szlenk. Entropy of piecewise monotone mappings. *Studia Mathematica*, 67:45–63, 1980.

[35] M.J.Feigenbaum. Quantitative universality for a class of nonlinear transformations. *J. Stat. Phys.*, 19(1):25–52, 1978.

[36] M.J.Feigenbaum. The universal metric properties of nonlinear transformations. *J. Stat. Phys.*, 21:669–706, 1979.

[37] M.J.Feigenbaum. Universal behavior in nonlinear systems. *Physica D*, 7:16–39, 1983.

[38] P. Myrberg. Sur l'itération des polynomes réels quadratiques. *J. Math. Pures Appl.*, 41(9):339–351, 1962.

[39] Diego F. M. Oliveira, Marko Robnik, and Edson D. Leonel. Shrimp-shape domains in a dissipative kicked rotator. *Chaos: An Interdisciplinary Journal of Nonlinear Science*, 21(4):043122, 2011.

[40] J. P. Eckmann P. Collet and H. Koch. Period doubling bifurcations for families of maps on r^n. *J. Stat. Phys.*, 25:1–14, 1981.

[41] Oleksandr Popovych, Valerii Krachkovskyi, and Peter Tass. Phase-locking swallows in coupled oscillators with delayed feedback. *Physical review. E, Statistical, nonlinear, and soft matter physics*, 82:046203, 10 2010.

[42] Joseph P. Previte and Kathleen A. Hoffman. Period doubling cascades in a predator-prey model with a scavenger. *SIAM Review*, 55(3):523–546, 2013.

[43] Laura M. Pérez, Jean Bragard, Hector Mancini, Jason A. C. Gallas, Ana M. Cabanas, Omar J. Suarez, and David Laroze. Effect of anisotropies on the magnetization dynamics. *Networks and Heterogeneous Media*, 10(1556-1801):209, 2015.

[44] C. Robinson. *An introduction to dynamical systems*. Prentice Hall, New Jersey, 2004.

[45] Jaime Rössler, Miguel Kiwi, Benno Hess, and Mario Markus. Modulated nonlinear processes and a novel mechanism to induce chaos. *Phys. Rev. A*, 39:5954–5960, June 1989.

[46] E. Sander and J. A. Yorke. Connecting period-doubling cascades to chaos. *International Journal of Bifurcation and Chaos*, 22(2), 2012.

[47] E. Sander and J.A. Yorke. Period doubling cascades galore. *Ergodic Theory and Dynamical systems*, 31(4):1249–1267, 2011.

[48] Evelyn Sander and J. A. Yorke. The many facets of chaos. *International Journal of Bifurcation and Chaos*, 25(4), 2015.

[49] Ruedi Stoop, Stefan Martignoli, Philipp Benner, Ralph Stoop, and Yoko Uwate. Shrimps: Occurrence, scaling and relevance. *International Journal of Bifurcation and Chaos in Applied Sciences and Engineering*, 22, 2012.

[50] Ilie Ugarcovici and Howard Weiss. Chaotic dynamics of a nonlinear density dependent population model. *Nonlinearity*, 17:1689–1711, 2004.

[51] Roxána Varga, Kálmán Klapcsik, and Ferenc Hegedűs. Route to shrimps: Dissipation driven formation of shrimp-shaped domains. *Chaos, Solitons and Fractals*, 130:109424, 2020.

[52] Renato Vitolo, Paul Glendinning, and Jason Gallas. Global structure of periodicity hubs in lyapunov phase diagrams of dissipative flows. *Physical review. E, Statistical, nonlinear, and soft matter physics*, 84:016216, 07 2011.

[53] J. A. Yorke and K. Alligood. Period doubling cascades of attractors: A prerequisite for horseshoes. *Comm. Math. Phys.*, 101(3):305–321, 1985.

[54] Y. Zou, M. Thiel, M. C. Romano, J. Kurths, and Q. Bi. Shrimp structure and associated dynamics in parametrically excited oscillators. *International Journal of Bifurcation and Chaos*, 16(12):3567–3579, 2006.

Curriculum Vitae

Vandana Saini received Bachelor of Science in Mathematics from Panjab University in 2006. She received Masters in Mathematics from Panjab University (2008) and Masters in Mathematics from George Mason University (2012). She is currently working as Mathematics Lecturer in Ocean County Community College in NJ.